BOSTON RESEARCH AND DEVELOPMENT LABORATORY

A C SPARK PLUG DIVISION

GENERAL MOTORS CORPORATION

WAKEFIELD, MASSACHUSETTS

ANALYSIS OF A PULSE RESTRAINED ACCELEROMETER

by

John C. Goclowski

August 1, 1962

Table of Contents

	Page
Chapter I - Introduction	1
Chapter II - System Description	5
2.1 Description of Accelerometer System	5
2.2 Pendulum Transfer Function	6
2.3 Periodicity of Limit Cycle	8
2.4 Normalization of Loop Parameters	9
Chapter III - Prediction of the Oscillatory Modes With Zero Input	10
3.1 Discussion of Nonlinear System Behavior	10
3.2 Methods of Analysis - Review of Literature	10
3.3 Describing Function Method	11
3.3.1 Describing Function of Contactor with Hysteresis	12
3.3.2. Effective Phase Shift of Sampler	13
3.3.3. Phase Angle vs. Log Frequency Curve	14
3.3.4. Effect of Sampling Rate on Moding	16
3.4 Piecewise Linear Analysis	18
3.4.1. Pendulum Dynamics During Limit Cycle	18
3.4.2. Pendulum Dynamics During Limit Cycle, Neglecting Elastic Restraint	20
3.4.3. Relating "Exact" Analysis and Describing Function Analysis	21
3.5 Analytic Mode Prediction	23
Chapter IV - System Response to Acceleration Inputs	26
4.1 Mode Switching Angle	26
4.2 Open Loop Response of Pendulum to Step Input	28
4.3 System Response to Step Input	28
4.4 Accelerometer Deadzone Due to Elastic Restraint	31
4.5 Mode Switching Without Producing Output	33
Chapter V - Accelerometer System Synthesis	35
5.1 General	35
5.2 Pendulosity	35
5.3 Torque Generator	35
5.4 Clock Frequency	36
5.5 Elastic Restraint	36
5.6 Pendulum Time Constant	36
Chapter VI -Conclusion and Recommendations	40
Appendix - Analog Computer Simulation	

Table of Figures

Figure

1.1 Pendulum Unit

2.1 Pulse Restrained Accelerometer System

2.2 Block Diagram of Pulse Restrained Accelerometer System

2.3 Simple Pendulum

3.1 Input-Output Characteristics of Contactor With Hysteresis

3.2 $-\frac{1}{G_D}$ and G_P vs. ω, 10 KC

3.3 $-\frac{1}{G_D}$ and G_P vs. ω, 2 KC

3.4 n vs. δ

3.5 2:2 and 3:3 Modes

3.6 Limit Cycle Frequency

4.1 Phase Plane Portrait, 2:2 and 3:3 Modes

4.2 Deadzone vs. Hysteresis

Table of Symbols

a	acceleration along input axis
C	damping constant
g	gravity
G_D	contactor describing function
G_P	pendulum transfer function
I	inertia of pendulum float
K	elastic restraint
K′	spring constant
m	dimensionless time $(\frac{t}{T})$
M	feedback torque
n:n	oscillatory mode having a periodic cycle consisting of n positive pulses followed by n negative pulses
P	pendulosity
s	Laplace Transform variable
S	Laplace Transform variable used with dimensionless time $(S = sT)$
t	time
T	interval between sample pulses
ΔV	increment of velocity
α	phase angle between $+\Delta\theta$ and $\theta_{n,o}$
β	ratio of pendulum time constant to integrator time constant $(\frac{T_2}{T_1})$
γ	ratio of sampling interval to pendulum time constant $(\frac{T}{T_2})$
δ	phase angle between $\theta = 0$ and $\theta_{n,o}$
θ	pendulum angle

θ'	dimensionless rate of change of θ per sampling interval ($\theta' = T\dot{\theta}$)
θ''	dimensionless second derivative of θ ($\theta'' = T^2\ddot{\theta}$)
θ_{ss}	steady-state pendulum angle
$\Delta\theta$	hysteresis angle
$\lvert\theta\rvert$	peak value of pendulum limit cycle oscillation
$\theta_{n,m}$	pendulum angle at the mth sample pulse after a torque reversal in an n:n mode
λ	$\frac{\pi}{n} - \alpha$
μ	dimensionless value of maximum rate of change of θ $\left[\mu = \frac{TM}{C}(1+\beta)\right]$
τ_1	integrator time constant ($\frac{C}{K}$)
τ_2	pendulum time constant ($\frac{I}{C}$)
ω	angular frequency

Analysis of a Pulse Restrained Accelerometer

Abstract

This report is concerned with the analysis of a pendulum torqued with pulses through the mechanism of a sample data contactor feedback loop. Such a system, called a pulse restrained accelerometer, can be used to provide incremental velocity information in an inertial navigation system.

The presence of the contactor causes the pendulum to oscillate continuously. The particular mode of oscillation (i.e., limit cycle frequency) depends on the loop parameters, initial conditions, hysteresis in the contactor and forcing functions. This report presents an analytic procedure for determining the oscillatory modes of the accelerometer for zero inputs and small acceleration step inputs.

A small amount of elastic restraint in the accelerometer, which can either be caused by gravitational force acting on the pendulum as it deflects from the vertical position or by a physical spring effect, will produce a deadzone within whose bounds input acceleration cannot be detected. This effect is also analyzed in this report.

CHAPTER 1

Introduction

The restrained pendulum accelerometer illustrated in Figure 1.1 has a cylindrical float supported concentrically in a sealed cylindrical case with a high density fluid filling the gap between the case and the float. The density of the fluid is such that the float is supported to neutral buoyancy; the output axis bearings serving mainly to center the float.

An unbalance mass is attached to the float rendering it pendulous, hence an acceleration applied along the input axis results in a deflection of the float about the output axis. Damping action is provided by the fluid. If the reference axis of the pendulum is oriented vertically, gravitational force acting upon the deflected pendulous mass will provide elastic restraint.

The deflection of the float about the output axis is detected by the signal generator and a feedback signal is provided to the torque generator which restores the accelerometer to its reference position. The feedback signal is, therefore, a measure of the acceleration input.

The accelerometer used in an inertial navigation system should accurately indicate the acceleration along its sensitive axis, of the vehicle in which it is mounted, over a measurement range of about 10^{-5} g's to 10 g's. The acceleration should also be in a form which can be readily integrated with respect to time to give vehicle velocity.

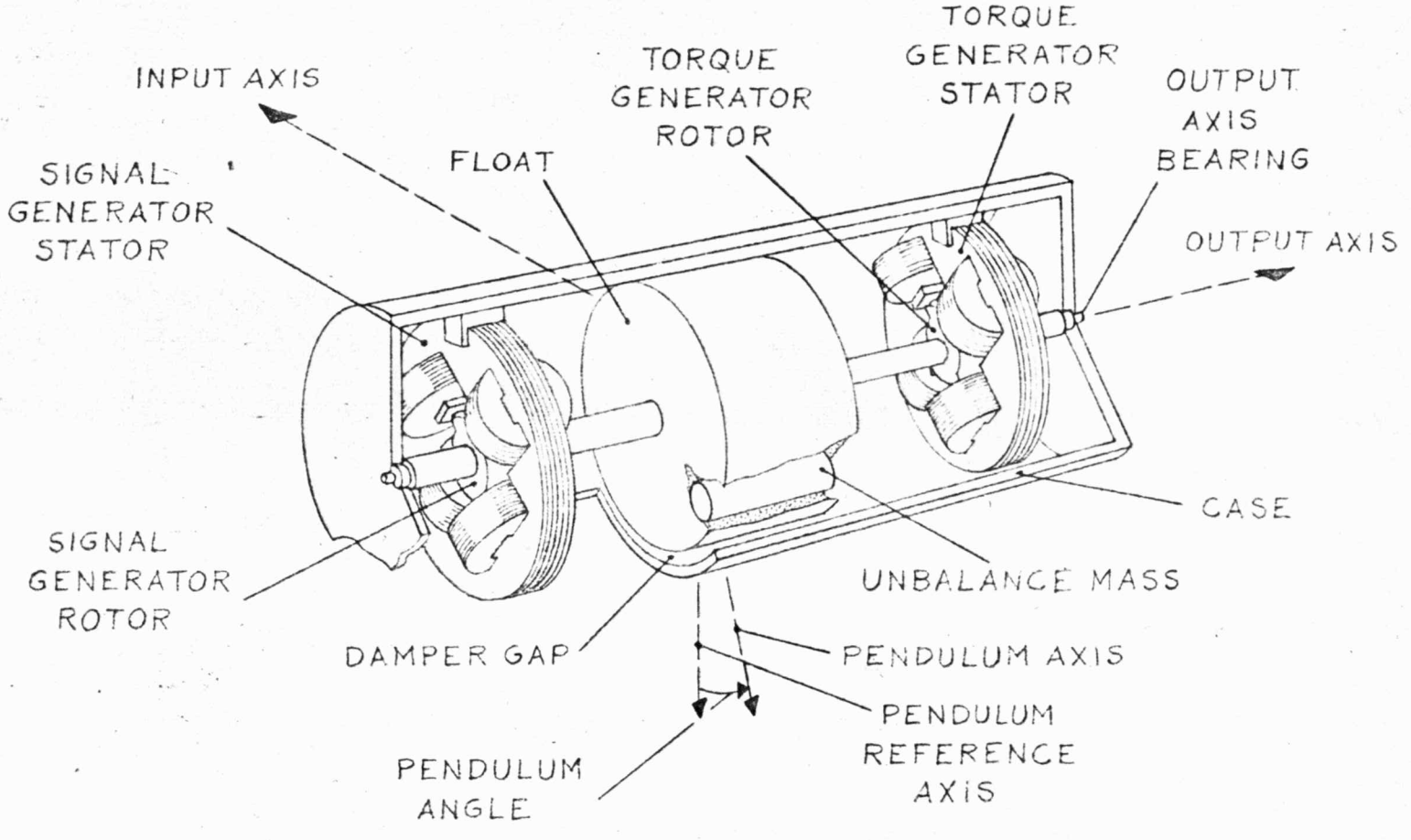

Fig. 1.1 PENDULUM UNIT

The feedback signal can either be in a digital form or in an analog form. The digital method has three distinct advantages.

1. It is desirable to measure the feedback signal to an accuracy of better than one part in 100,000. This exceeds the capability with which most analog quantities can be readily measured. Since time can be measured more accurately than most analog quantities, the digital method consists of discrete time measurements and counting. The accelerometer which has a feedback signal consisting of positive and negative pulses of constant magnitude and of discrete duration is called a pulse restrained accelerometer and the analysis of such a system is the subject of this report. An open-loop analog-to-digital conversion of the analog feedback signal would not improve the accuracy because the conversion still requires the measurement of an analog quantity other than time.
2. Since the pulses would be of constant amplitude in the digital method, there would be no need for a linear torque generator and power amplifier; instead, only a constant current supply would be required. The measurement of the feedback torque would be easily achieved over the desired range with such an accelerometer since it would not exhibit the nonlinear characteristics typical of electromagnetic devices.
3. The amplitude of pulses, M, is proportional to a constant amount of input acceleration. Since the pulse duration, T, is also a constant; then each pulse is proportional to an increment of velocity, ΔV, where

$\Delta V = MT$. The process of integrating acceleration now consists of merely counting the pulses which represent the incremental velocity. Generally, the integration in the analog system is accomplished with a motor-tachometer combination. The accuracy of this method is limited by the tachometer null characteristics and the linearity of the motor, tachometer, and drive amplifier.

One other possible advantage of the pulse restrained pendulum is that the limit cycle oscillation can provide the "dithering" required to overcome any static friction which may be present in the system. On the other hand, a disadvantage of the digital system is that the presence of an elastic restraint torque may prevent the pendulum from attaining the angle required in order to produce a sensible output in response to an acceleration input. Fortunately, this deadzone can be reduced to a negligible value by increasing the sampling frequency.

The pulse restrained accelerometer with its nonlinear feedback control system is potentially more accurate and less complex than the accelerometer which incorporates a linear feedback control system. In order to realize the maximum capabilities of such a system this report develops, through the application of various nonlinear techniques, procedures for predicting the dynamic behavior of a pulse restrained accelerometer system. The main purpose of this report is to (1) present a method for determining the oscillatory modes (i.e., limit cycles) which exist during zero and small

input conditions and (2) determine the deadzone resulting from the presence of elastic restraint in the system.

The following chapter contains a description of a pulse restrained accelerometer and a development of the basic equations of the system.

In Chapter III, the sample data contactor feedback control system of the pulse restrained accelerometer is analyzed by the phase plane method, the describing function method and a piecewise linear analysis method for zero input acceleration.

In Chapter IV, the response of the system to step inputs is discussed. The performance of the system is predicted by a heuristic extension of the analysis in Chapter III since no rigorous technique exists for the transient analysis of a sample data contactor feedback control system. The results of the analysis are supplemented by an analog computer simulation and some laboratory tests with an experimental accelerometer.

Based upon the analysis, design criteria for the synthesis of a pulse restrained accelerometer are presented in Chapter V.

The final chapter presents the conclusions of the investigation and recommendations for further study.

CHAPTER II

System Description and Equations

2.1 Description of Accelerometer System

The complete pulse restrained accelerometer system is shown in Figure 2.1. Under the influence of an input acceleration, a, the pendulum rotates from its reference position. The output of the signal generator indicates the angle of the pendulum, θ. When the pendulum angle exceeds a threshold angle, $\Delta\theta$, the polarity switch changes to the opposite state. At the next sampling instant, the state of the torque switch changes and gates the constant current source in the opposite direction through the torque generator. The sense of the torque generator output is such that it tends to drive the pendulum back to its reference position.

In addition to gating the sense of the constant current source to the torque generator, the torque switch also gates the clock pulses to the up-and-down counter. The contents of the up-and-down counter are periodically transferred to an accumulator and the counter is reset to zero. The up-and-down counter essentially acts as a filter which removes the limit cycle oscillation from the velocity information.

Since the feedback torque does not have a zero state (i.e., its only output is $\pm$ M), the steady state condition of the accelerometer loop is a continuous self-sustained oscillation of some definite amplitude and frequency. The presence of sampling and hysteresis in the loop tends to increase the amplitude of the "hunting" or limit cycling. Typical waveforms generated in the system during the limit cycling are also shown in Figure 2.1.

When the pendulum experiences an acceleration input, the time required for the pendulum to swing on one side of its reference position is longer than

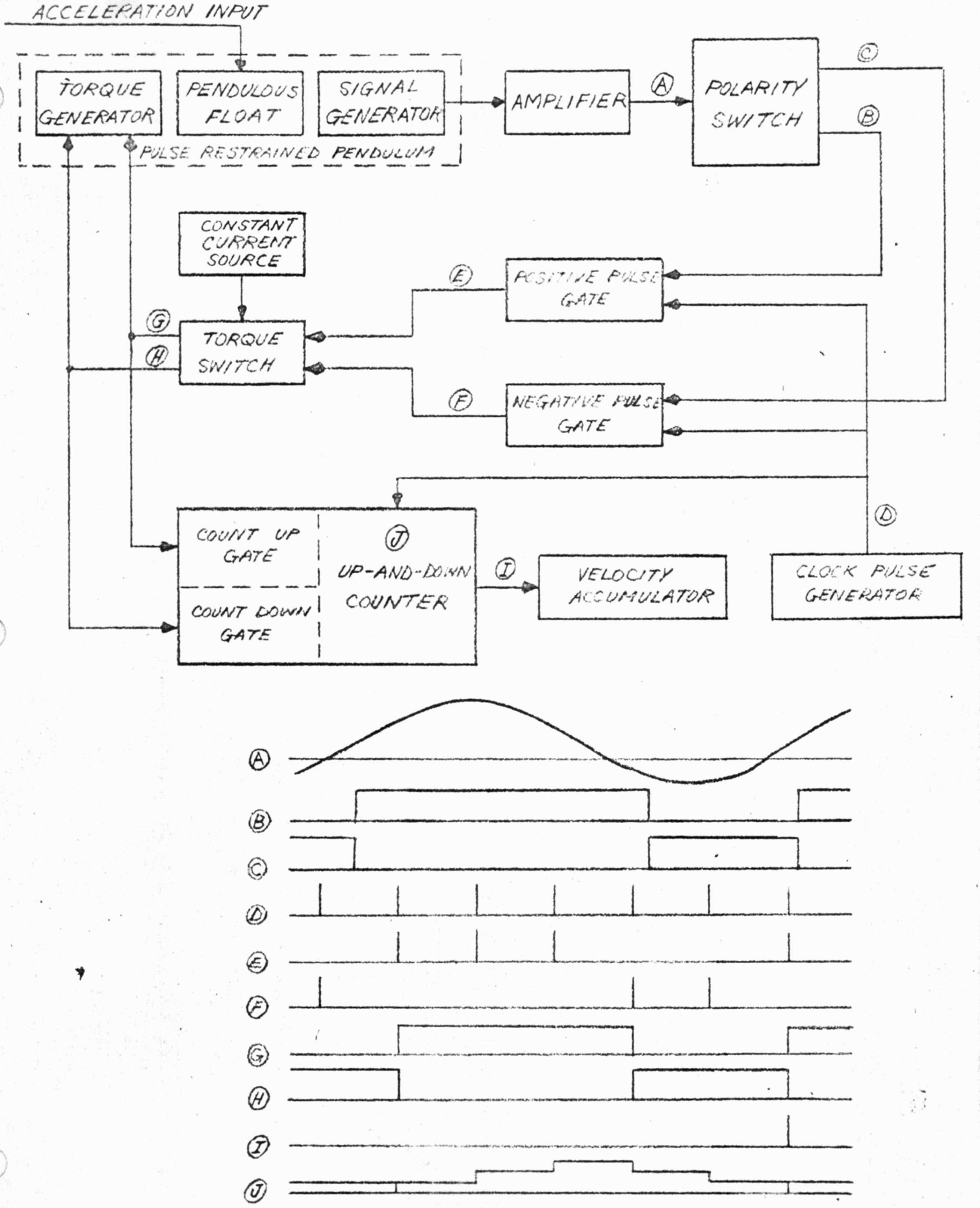

Fig. 2.1 PULSE RESTRAINED ACCELEROMETER SYSTEM

the time required to swing on the other side. Therefore, the number of sampling pulses existing during one half of a torque cycle exceeds those existing during the other half cycle. The difference between the number of sampling pulses in the two half cycles is proportional to the change in the vehicle velocity.

A simplified block diagram of the accelerometer system is shown in Figure 2.2. The polarity switch of Figure 2.1 is represented by the contactor which has an input-output characteristic that includes hysteresis. This hysteresis results from the fact that some finite deflection of the pendulum is required to trigger the polarity switch. Generally the sensitivity of the signal generator is not increased beyond the point where the polarity switch is triggered by noise. The sampler represents the positive and negative pulse gates. The torque switch provides the feedback gain while also acting as a zero order hold following the sampler.

The fact that the pendulum is not at its reference position at the end of the torque cycle constitutes an instantaneous velocity error. The velocity error is bounded by the "self-correcting" action of the feedback loop so that this portion of the velocity information is not lost but rather it just temporarily stored in the pendulum position.

2.2 Pendulum Transfer Function

The acceleration sensing instrument can be considered as consisting of the simple pendulum shown in Figure 2.3. The moment of inertia I is the polar mement of inertia of the float and pendulous mass about the output axis which is directed into the plane of the paper. The damping coefficient C is afforded by the fluid separating the case and the float. The elastic restraint

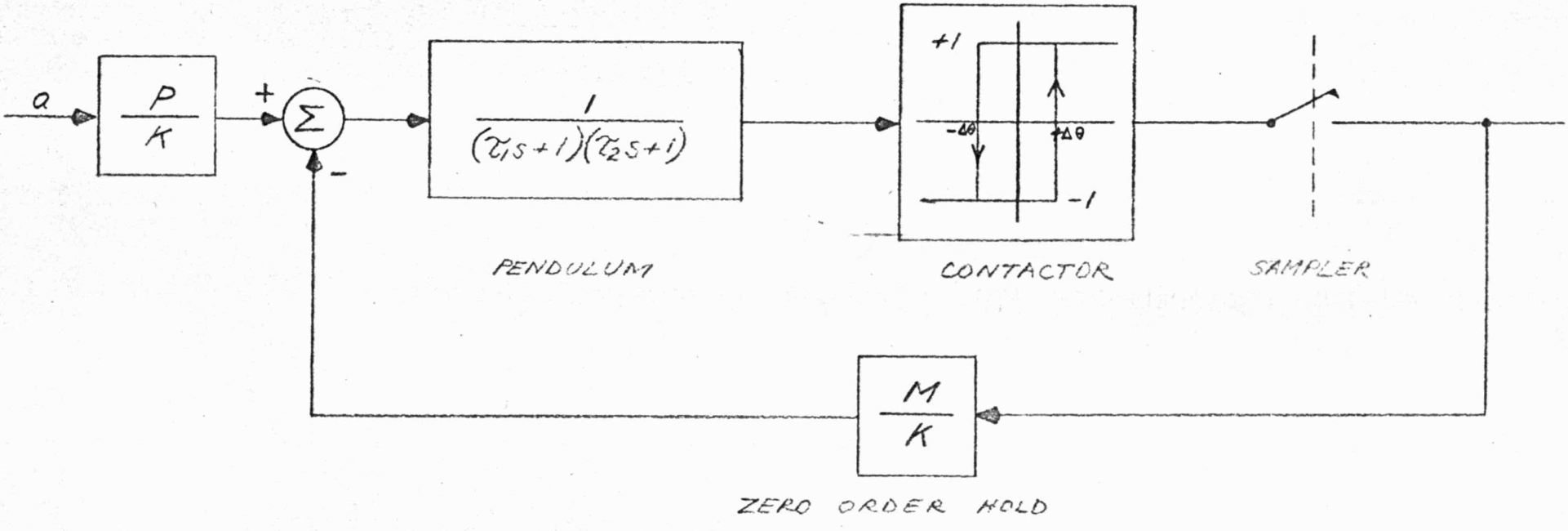

Fig. 2.2 BLOCK DIAGRAM OF PULSE RESTRAINED ACCELEROMETER SYSTEM

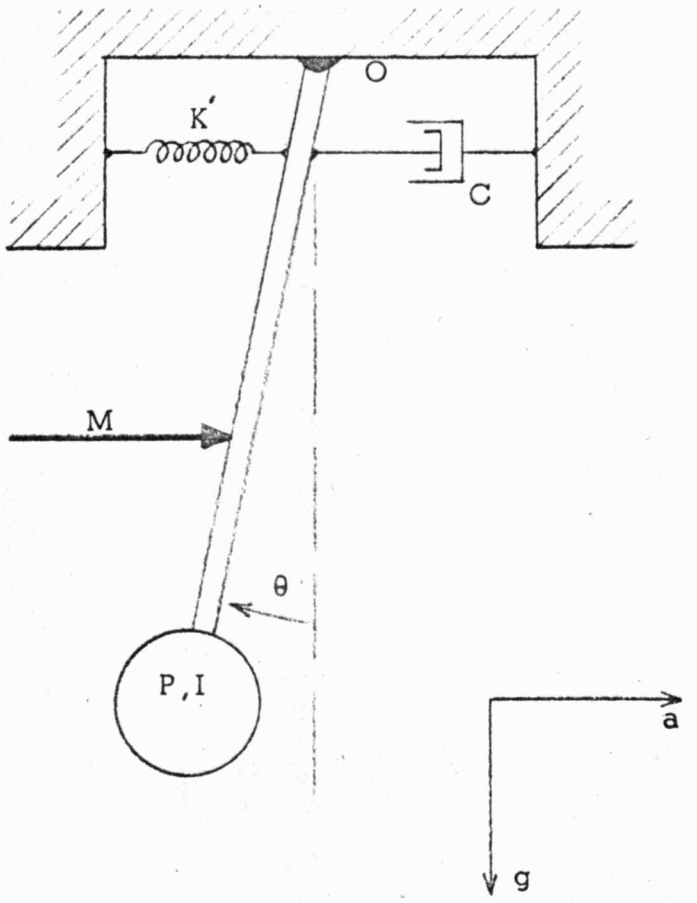

I = moment of inertia
C = damping coefficient
K′ = spring constant
M = applied torque
P = pendulosity
a = acceleration
g = gravity
θ = angular displacement of pendulum

Fig. 2.3 Simple Pendulum

K may exist in the system (1) due to the presence of a spring with a spring constant K′ or (2) if the instrument is oriented such that the gravitational acceleration acts upon the pendulous mass P of the deflected pendulum to produce the restraining torque $Pg \sin\theta$. The feedback torque during a torque half cycle is constant and in a direction such that it tends to drive the pendulum toward its reference position (i.e., $\theta = 0$). Therefore, the pendulum dynamics during a torque half cycle can be described by a linear differential equation.

Applying the rotational form of Newton's second law to the pendulum in Figure 2.3, the rate of change of the angular momentum is equal to the summation of torques about the pivot 0.

$$I\ddot{\theta} = \sum \text{torques} \qquad 2.1$$

$$= -C\dot{\theta} - K'\theta - Pg\sin\theta + Pa\cos\theta \pm M \qquad 2.2$$

When the accelerometer is operating in a closed loop fashion, the pendulum remains in the vicinity of its reference position and small angle approximations can be made (i.e., $\sin\theta = \theta$, $\cos\theta = 1$). Letting $K' + P_g = K$, the total elastic restraint, equation 2.2 can be written as follows during the interval where θ is positive:

$$\ddot{\theta} + \frac{C}{I}\dot{\theta} + \frac{K}{I}\theta = \frac{Pa}{I} - \frac{M}{I} \qquad 2.3$$

Considering the feedback torque M as being of constant magnitude and sign, the Laplace transform of equation 2.3 from the t-domain into the s-domain is:

$$\left(s^2 + \frac{C}{I}s + \frac{K}{I}\right)\theta_{(s)} = \frac{P}{I}a_{(s)} - \frac{M}{sI} + \dot{\theta}_o + \left(s + \frac{C}{I}\right)\theta_o \qquad 2.4$$

The left member of equation 2.4 can be factored and the equation can

be written in terms of the time constants τ_1, and τ_2 as follows:

$$\theta_{(s)} = \frac{\frac{P_{a(s)}}{\tau_1 \tau_2 K} - \frac{M}{s(\tau_1+\tau_2)C} + \dot{\theta}_o + \left(s + \frac{1}{\tau_1+\tau_2}\right)\theta_o}{\left(s+\frac{1}{\tau_1}\right)\left(s+\frac{1}{\tau_2}\right)} \qquad 2.5$$

$$\text{where } \tau_1 = \frac{2\frac{I}{C}}{1-\left[1-\frac{4KI}{C^2}\right]^{\frac{1}{2}}}, \quad \tau_2 = \frac{2\frac{I}{C}}{1+\left[1-\frac{4KI}{C^2}\right]^{\frac{1}{2}}}$$

In most cases, we find

$$\frac{4KI}{C^2} \ll 1, \quad \therefore \left[1-\frac{4KI}{C^2}\right]^{\frac{1}{2}} \approx 1 - \frac{2KI}{C^2} + \ldots\ldots$$

and the time constants can be approximated as

$$\tau_1 \approx \frac{C}{K} \qquad \text{(integrator time constant)}$$

$$\tau_2 \approx \frac{I}{C} \qquad \text{(pendulum time constant)} \qquad 2.6$$

2.3 Periodicity of Limit Cycle

Since the torque switch output cannot be zero, the pendulum output cannot remain at zero at all times. Therefore, the response of the system to zero acceleration inputs is such that the average value of both, the pendulum and the torque switch, is zero.

From the standpoint of symmetry, the torque switch output must be a square wave and the pendulum output must be the response of the pendulum to this square wave. Since the torque switch can change state only when a clock pulse is gated to its input, the square wave output of the torque switch is constrained to have a period which is an integer multiple of the sampling period, 2T (T is the time interval between sampling pulses).

The self-sustaining oscillation of the pendulum in the closed loop is known as a limit cycle. The torque feedback signal, however, has a period which consists of n positive pulses followed by n negative pulses. The cyclic characteristic of the loop operation will be referred to in this report as being an n:n mode. The term $\theta_{n,m}$ will signify the pendulum angle at the mth sampling instant of a torque half cycle which has a duration of n pulses.

2.4 Normalization of Loop Parameters

It is convenient in the derivation of general equations which describe the dynamic behavior of the pendulum to normalize time with respect to the sampling interval, T. Using T as the basis time unit, the following dimensionless quantities are defined.

$m = \frac{t}{T}$ (dimensionless time)

$\frac{1}{\gamma} = \frac{\tau_2}{T}$ (dimensionless pendulum time constant)

$\frac{1}{\beta\gamma} = \frac{\tau_1}{T}$ (dimensionless integrator time constant)

$\theta' = T\dot{\theta}$ (dimensionless time derivative of θ)

$\theta'' = T^2\ddot{\theta}$ (dimensionless second time derivation of θ)

$\mu = \frac{TM}{C}(1+\beta)$ dimensionless value of maximum rate of change of θ)

CHAPTER III

Prediction of the Oscillatory Modes with Zero Input

3.1 Discussion of Non-linear System Behavior

The response of a linear system can be determined by obtaining the inverse Laplace transform. After the transient response due to the initial conditions and forcing functions has decayed exponentially to a negligible value, there exists the steady state response which is independent of initial conditions. A non-linear system with a saturating element (i.e., a contactor) can be considered as having a variable gain.[1*] The loop "gain" approaches infinity for small amplitude oscillations and becomes low for large amplitude oscillations. Depending on the order of the system, small oscillations(high gain) could be unstable and would grow larger while large oscillations (low gain) could be stable and would grow smaller. In between these extremes there would be an amplitude of oscillation just small enough to give the value of gain required to keep the system on the verge of instability. The system will eventually settle down into this so-called limit cycle, independent of the initial conditions.

Sample data contactor feedback control systems can exhibit the property of having more than one limit cycle. As a result, when an input is applied, the system steady-state response can be different, depending on the initial conditions.

3.2 Methods of Analysis-Review of Literature

The first approach to determining the dynamic behavior of contactor servos was the use of the classical differential equation by Hazen.[2] Laplace transform theory was applied by Kahn[3] to develop a semigraphical method of solution for

*Superscripts refer to the bibliography at the end of the report.

determining the transient behavior, relative stability, and oscillatory condition of the non-linear contactor servo. Bergen[4] adds to the use of the Z-transform to this type of piecewise linearization to account for the presence of a sampler in the loop. A similar approach is the method proposed by Torng and Meserve[5] using difference equations.

Weiss[6] and McColl[7] applied the phase plane method employed by Minorsky[8] and by Andronow and Chaikin[9] in other problems concerning nonlinear systems. In more recent years, the combination of sample data and contactors in a nonlinear system have been analyzed by Kalman[10] and by Mullin and Jury[11] with the use of the phase plane.

The describing function technique developed by Kochenburger[12] has been employed by Chow[13], Chao[14], and Gelb[15] to present a graphical representation of the contactor servo.

All three general analytic methods: piecewise linearization, phase plane analysis and describing function analysis will be used to investigate the behavior of the sample data contactor feedback control system. Although each method has its limitations, some insight is contributed by each to a better understanding of the nonlinear system. In this report, the various portions of the system analysis will be performed in each case, by the most suitable method available.

The bibliography at the end of this report should provide sufficient information to indicate the major work done in this field of sample data contactor servo analysis.

3.3 Describing Function Method

The first method of analysis to be used in this report is the describing

function technique because of its simplicity. The various modes of oscillation which can possibly exist are readily determined by this method.

3.3.1. Describing Function of Contactor with Hysteresis

The contactor will invariably have some hysteresis associated with it because the gain of the amplifier which drives the polarity switch in Figure 2.1 is normally never increased beyond the point where the polarity switch is triggered by the noise present in the signal generator output.

The describing function for the nonlinear element shown in Figure 3.1 is:

$$G_D = \frac{4}{\pi|\theta|} \angle \sin^{-1} \frac{\Delta\theta}{|\theta|} \qquad 3.1$$

where the gain of the contactor is the ratio of the fundamental component of the square wave output, $\frac{4}{\pi}$, to the amplitude of the sinusoidal input, $|\theta|$. The phase shift contributed by the hysteresis is $-\sin^{-1}\frac{\Delta\theta}{|\theta|}$.

The basic assumption of the describing function method, that only the fundamental of the output need be considered, is a valid one for two reasons: (1) the frequency spectrum of a square wave consists of progressively smaller amplitudes for increasing order of the harmonic frequency components and (2) the pendulum acts as a low pass filter to the square wave so that the signal fed back to the input of the nonlinear element is essentially sinusoidal.

The quasi-linearization by means of the describing function allows the frequency response of the accelerometer system shown in Figure 2.2 to be approximated by:

$$\frac{\theta(j\omega)}{a(j\omega)} = \frac{G(j\omega)G_D}{1 + G(j\omega)G_D} \qquad 3.2$$

where G_D = describing function

$G(j\omega)$ = frequency sensitive portion of system

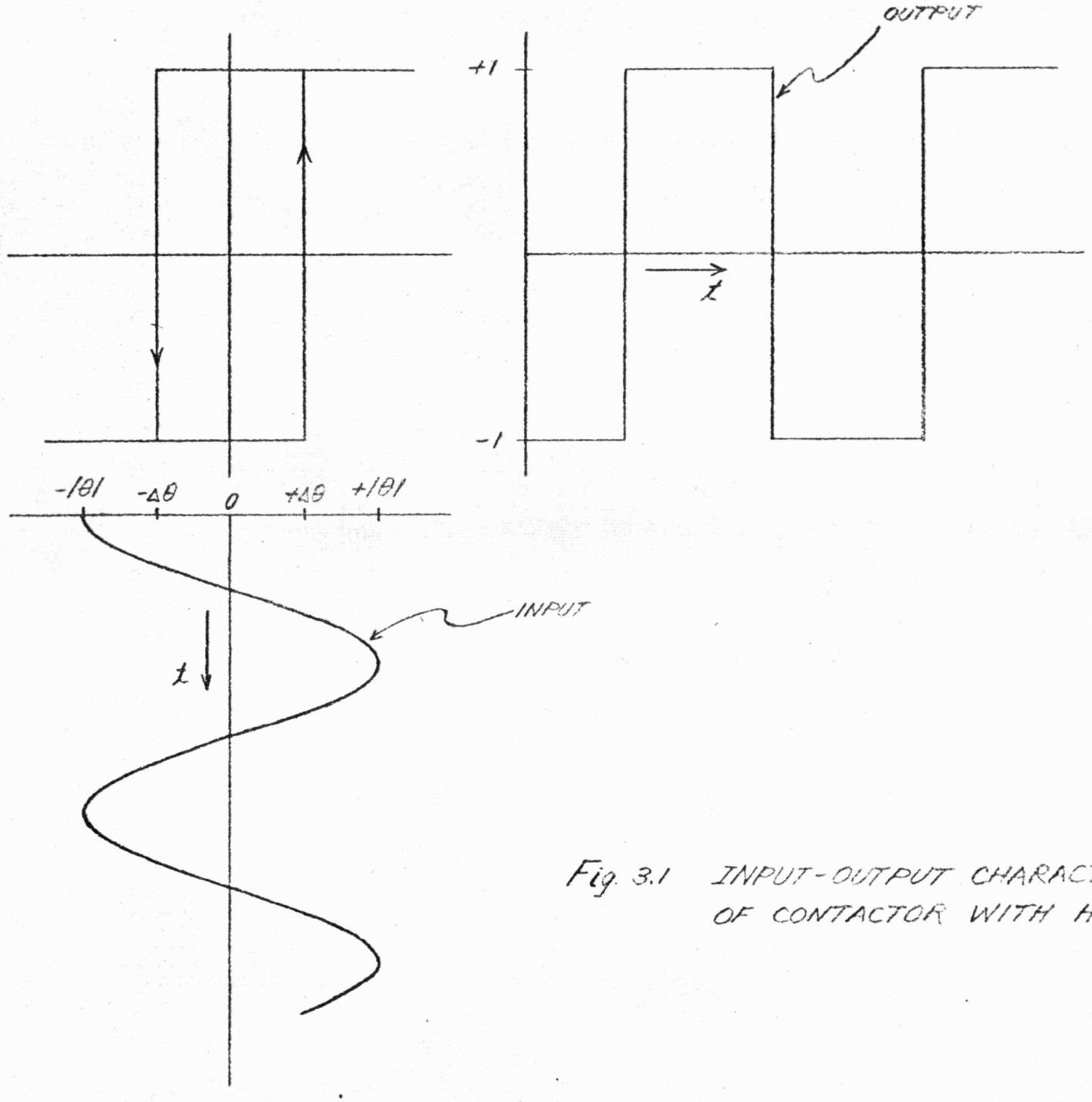

Fig. 3.1 INPUT-OUTPUT CHARACTERISTICS OF CONTACTOR WITH HYSTERESIS

The system will be critically stable in a particular n:n mode when the denominator is zero or i.e., when

$$-\frac{1}{G_D} = G(j\omega) \qquad 3.3$$

When equation 3.3 is satisfied, the system will have a sustained oscillation of the amplitude and frequency which satisfy the equation. The intersections of $-\frac{1}{G_D}$ and $G(j\omega)$ on a log magnitude-angle diagram would indicate the oscillatory modes which are possible in the system. $G(j\omega)$ would include the pendulum and the effective phase shift of the sampler while, according to equation 3.1,

$$-\frac{1}{G_D} = \frac{\pi|\theta|}{4} \angle 180^\circ - \sin^{-1}\frac{\Delta\theta}{|\theta|} \qquad 3.4$$

A plot of log $|\theta|$ versus phase-shift as a function of frequency would be very useful, particularly if the variation of the pendulum parameters or the effect of compensation were to be investigated. However, if the linear portion of the loop is assumed to remain fixed, a simpler plot of phase shift vs. log frequency can be used to determine the moding characteristics.

3.3.2. Effective Phase Shift of Sampler

An effective phase shift can be ascribed to the sampler when the accelerometer loop, shown in Figure 2.1, is operating in a particular n:n mode of oscillation. The sampler represents the gates which exist between the polarity switch and the torque switch. The outputs of the two switches are square waves having the same period.

There can be a delay between the time the polarity switch changes its state and the time when the next clock pulse is gated to the torque switch to change its state. This time delay between the outputs of the two switches would be zero if the clock pulse was gated to the torque switch immediately after the

polarity switch changed state. If the polarity switch changed state immediately after a clock pulse, there would be a time delay equal to one sample interval, T, before the torque switch changed state. Thus, the length of the time delay is between 0 and T seconds.

In the describing function analysis to follow, the feedback torque being applied to the pendulum will be considered as consisting of only the fundamental component of the square wave. In this regard, a time delay of T seconds between the two switch outputs during an n:n mode of oscillation can be considered as a phase shift of $\frac{\pi}{n}$ degrees between the fundamental components of the outputs.

3.3.3. Phase Angle vs. Log Frequency Curve

The expression for the response of the linear portion of the system to a sinusoid according to Figure 2.2, is:

$$\frac{\frac{M}{K}}{(j\omega\tau_1+1)(j\omega\tau_2+1)}$$

Therefore, the phase shift due to the pendulum is:

$$\phi_{PENDULUM} = -\tan^{-1}\omega\tau_1 - \tan^{-1}\omega\tau_2 \qquad 3.5$$

The possible effective phase shift of the sampler was shown in section 3.3.2 to be:

$$0 \leq \phi_{SAMPLER} \leq \frac{\pi}{n} \qquad 3.6$$

The phase angle of $-\frac{1}{G_D}$ according to section 3.3.1., is

$$\phi_{-\frac{1}{G_D}} = 180^\circ - \sin^{-1}\frac{\Delta\theta}{|\theta|} \qquad 3.7$$

$$\text{where } |\theta| = \frac{\frac{M}{K}}{\left[1+\omega^2\tau_1^2\right]^{\frac{1}{2}}\left[1+\omega^2\tau_2^2\right]^{\frac{1}{2}}} \qquad 3.8$$

The experimental accelerometer used in the laboratory tests supporting this analysis has the following parameters:

$$\tau_1 = \frac{C}{K} = 12.5 \text{ sec}$$
$$\tau_2 = \frac{I}{C} = 43\times10^{-3} \text{ sec}$$
$$\frac{K}{P_g} = 9 \text{ where } K = P_g + K' \qquad 3.9$$
$$M = 5P_g$$
$$\Delta\theta = \text{system variable}$$
$$T = \text{system variable}$$

The phase angles given by equations 3.5, 3.6, and 3.7 are shown in Figure 3.2 for the parameters in equations 3.9 and various valuesof $\Delta\theta$. Since the clock pulse rate is 10^4 pps, $T = 10^{-4}$ sec. Although the pendulum phase shift curve is continuous over the entire frequency spectrum, the presence of the sampler constrains the modes of oscillation to be n:n modes where n is an integer. Since the period of an n:n mode is 2nT seconds, the frequency of an n:n mode is:

$$\omega_{n:n} = \frac{\pi}{nT} \qquad 3.10$$

The possible effective phase shift which can be contributed by the sampler can range from 0 to $\frac{\pi}{n}$ radians. The maximum value is shown in Figure 3.2. The actual amount of phase shift can be determined from the intersection of $\phi_{G(j\omega)}$ and $\phi_{-\frac{1}{G_D}}$.

For the case where $\Delta\theta$ = 1 second of arc, the 9:9 and 10:10 modes of oscillation are both possible. The initial conditions and the interval between the time the loop was closed and the time that the first clock pulse appeared determined which of the two possible modes would be attained in the steady-state condition. The data obtained from the laboratory experiments and the analog computer simulation agreed very well with this graphical prediction of the possible modes.

Figure 3.3 shows the phase angle curves which exist when the clock pulse rate is 2×10^3 pps. The change from 10^4 pps to 2×10^3 pps clock rate results in changes of the effective phase shift of the sampler and the possible limit cycle frequencies. The 2:2 and 3:3 modes are possible when the hysteresis is $\pm$ 1 second of arc.

The oscillatory modes which are capable of being sustained by the accelerometer loop have been determined by (1) assuming the existance of a particular oscillatory mode at the output, (2) following the signal around the loop, account-

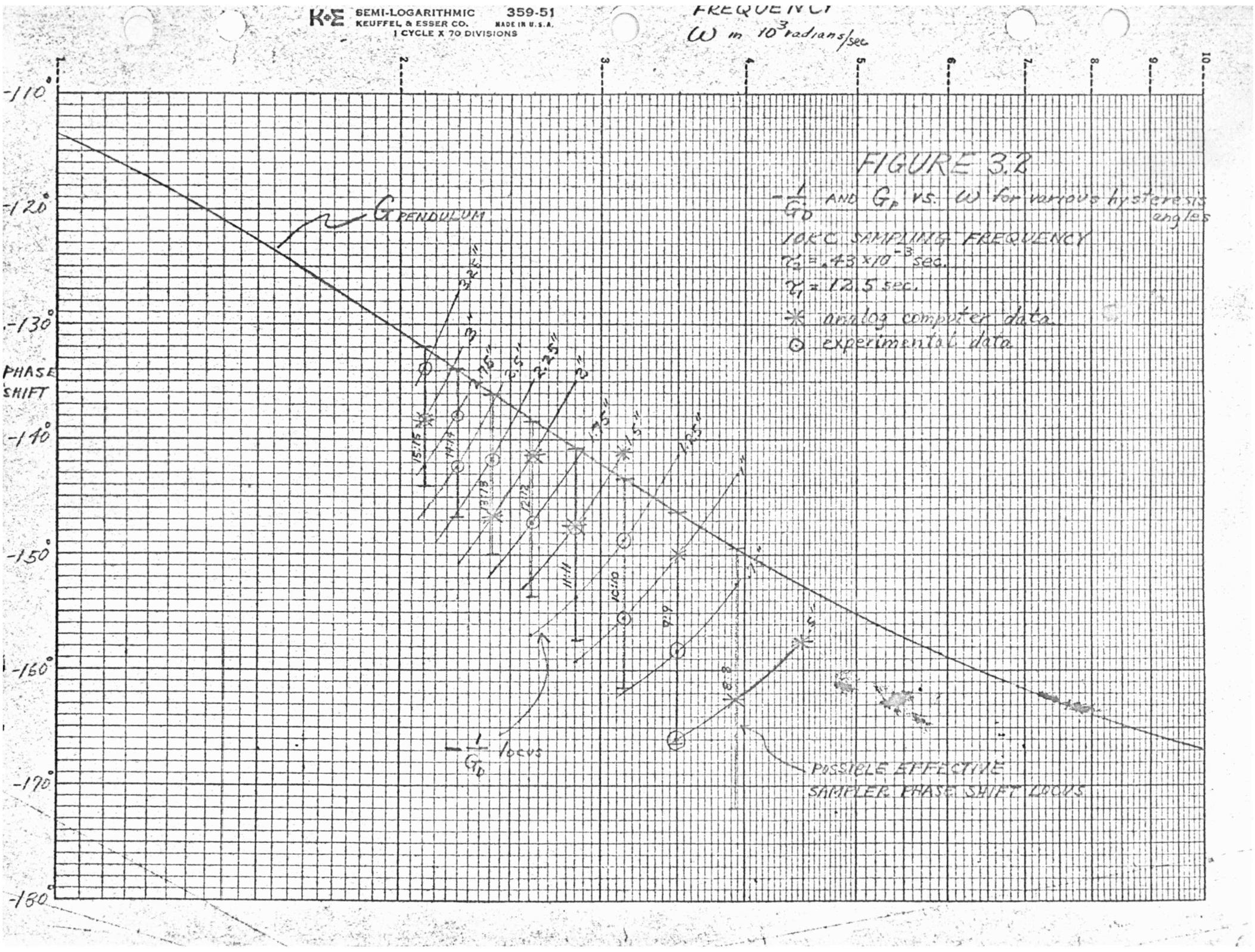
K&E SEMI-LOGARITHMIC 359-51
KEUFFEL & ESSER CO. MADE IN U.S.A.
1 CYCLE X 70 DIVISIONS
FREQUENCY
ω in 10^3 radians/sec
1
2
3
4
5
6
7
8
9
10
-110°
-120°
-130°
PHASE SHIFT
-140°
-150°
-160°
-170°
-180°
G PENDULUM
FIGURE 3.2
-1/G_D AND G_P VS. ω for various hysteresis angles
10 K'C SAMPLING FREQUENCY
τ2 = .43 x 10^-3 sec.
τ1 = 12.5 sec.
* analog computer data.
⊙ experimental data.
3.2°
3°
2.75°
2.5°
2.25°
2°
1.75°
1.5°
1.25°
1°
.75°
.5°
15.15
14.14
13.13
12.12
11.11
10.10
9.9
8.8
-1/G_D locus
POSSIBLE EFFECTIVE SAMPLER PHASE SHIFT LOCUS

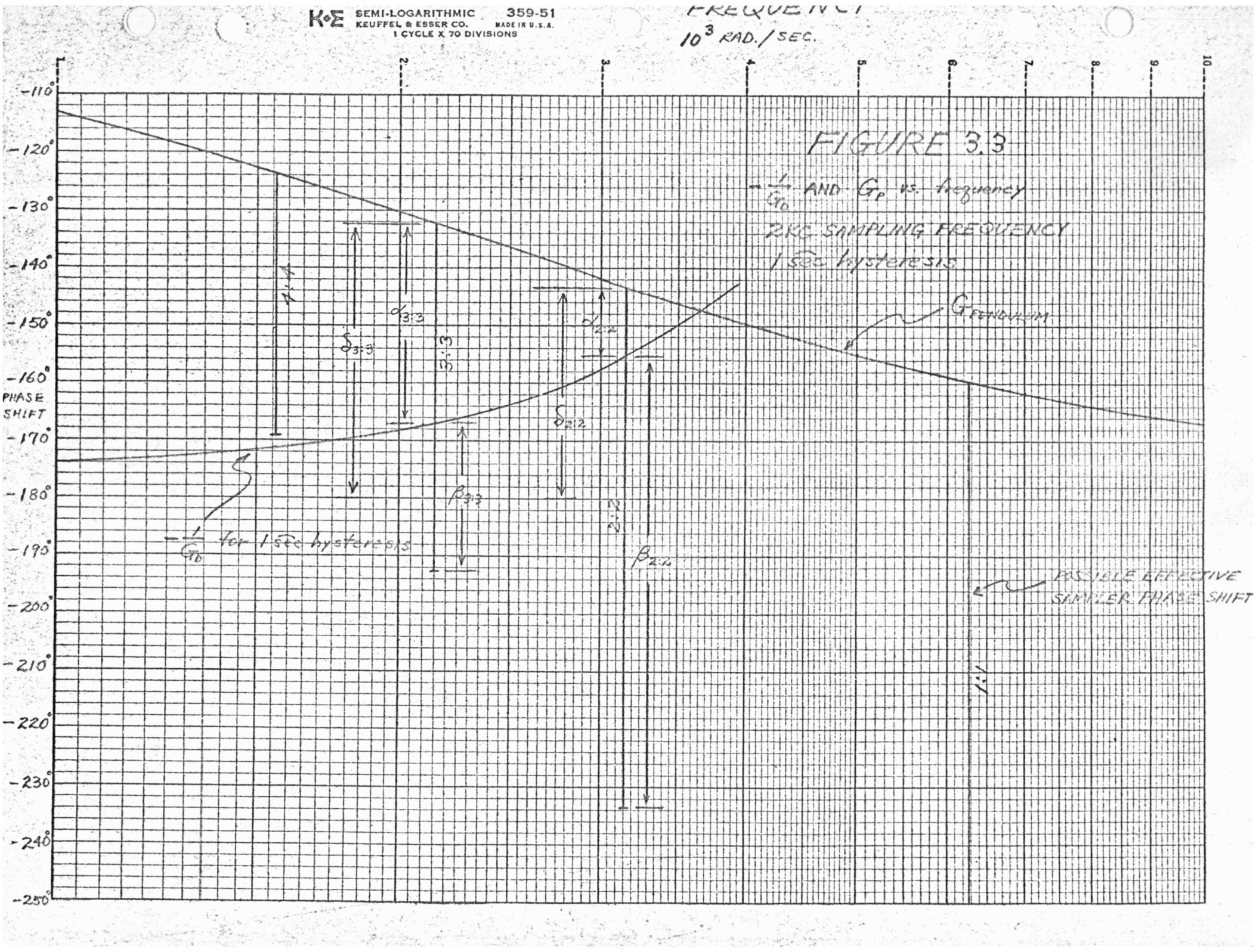
K·E SEMI-LOGARITHMIC 359-51
KEUFFEL & ESSER CO. MADE IN U.S.A.
1 CYCLE X 70 DIVISIONS
FREQUENCY
10^3 RAD./SEC.
1
2
3
4
5
6
7
8
9
10
-110°
-120°
-130°
-140°
-150°
-160°
PHASE SHIFT
-170°
-180°
-190°
-200°
-210°
-220°
-230°
-240°
-250°
FIGURE 3.3
-1/G_D AND G_P VS. FREQUENCY
2KC SAMPLING FREQUENCY
1 SEC HYSTERESIS
G_PENDULUM
δ3:3
α3:3
β3:3
δ2:2
α2:2
β2:2
-1/G_D for 1 sec hysteresis
POSSIBLE EFFECTIVE SAMPLER PHASE SHIFT

ing for all possible phase shift, and (3) observing whether enough phase shift is provided for the particular n:nmode to be sustained. The effect of amplitude change as the signal is followed around the loop is not considered since the sampler output is a function of only the polarity of the pendulum output. In this regard, the 4:4 mode is shown to be impossible in Figure 3.3 because insufficient phase shift is provided. In this particular case, the 1:1 mode is impossible, not because of too much phase shift but rather because the $-\frac{1}{G_p}$ curve never reaches the 1:1 frequency indicating that the amplitude of the 1:1 mode is less than 1 second of arc.

3.3.4. Effect of Sampling Rate on Moding

The highest possible mode of oscillation in the system without any contactor hysteresis occurs when the pendulum phase shift and the maximum effective phase shift of the sampler equal $-\pi$ radians, according to Figure 3.3.

Thus,
$$\tan^{-1}-\omega\tau_1 + \tan^{-1}-\omega\tau_2 - \frac{\pi}{n} = -\pi \qquad 3.11$$

Normalizing $\omega\tau_1$ and $\omega\tau_2$, equation 3.11 can be written as:

$$\tan^{-1}\frac{-\pi}{\beta\gamma n} + \tan^{-1}\frac{-\pi}{\gamma n} = -\pi + \frac{\pi}{n} \qquad 3.12$$

Since the summation of angles in the right member of equation 3.12 equals the summation of angles in the left member, the tangents of the two members are also equal.
$$\tan\left(\tan^{-1}\frac{-\pi}{\beta\gamma n} + \tan^{-1}\frac{-\pi}{\gamma n}\right) = \tan\left(\frac{\pi}{n} - 180^\circ\right) = -\tan\frac{\pi}{n} \qquad 3.13$$

Using the trignometric identity

$$\tan(x+y) = \frac{\tan x + \tan y}{1 - \tan x \tan y}$$

equation 3.13 can be written as follows:

$$\frac{\frac{\pi}{\beta\gamma n} + \frac{\pi}{\gamma n}}{1 - \frac{\pi^2}{n^2\gamma^2\beta}} = \tan\frac{\pi}{n}$$

Regrouping yields

$$\gamma^2 - \frac{\gamma\pi(1+\beta)}{n\beta\tan\frac{\pi}{n}} - \frac{\pi^2}{n^2\beta} = 0 \qquad 3.14$$

Solving for γ in equation 3.14 ,

$$\gamma = \frac{-\pi(1+\beta)}{2n\beta \tan\frac{\pi}{n}} \left[1 - \left(1 + \frac{4\beta \tan^2 \frac{\pi}{n}}{(1+\beta)^2} \right)^{\frac{1}{2}} \right] \qquad 3.15$$

Equation 3.15 is the expression for the largest value of γ which will allow a particular n:n mode to be self sustaining in a loop without hysteresis. Since $\gamma = \frac{T}{\tau_2}$, it follows that a decrease in the sampling frequency (i.e., an increase in T) or a shorter pendulum time constant would cause this n:n mode to be incapable of being sustained. Only lower values of n would then be possible.

On the basis of equation 3.15, the possible modes are plotted as a function of γ in Figure 3.4 . For n=1, $\tan\frac{\pi}{n}=0$ and the denominator of the right member of equation 3.15 must equal zero. Therefore, the largest value of γ for n = 1 is ∞, which means that the 1:1 mode is possible at all sampling frequencies. For n = 2, $\tan\frac{\pi}{n}=\infty$ and the middle term of the left member of equation 3.14 must equal zero and

$$\gamma = \frac{\pi}{2\sqrt{\beta}} \qquad (\text{for } n=2) \qquad 3.16$$

For $n \geq 3$, the quantity under the radical sign in equation 3.15 can be approximated by the first two terms of the series expansion:

$$\left(1 + \frac{4\beta \tan^2 \frac{\pi}{n}}{(1+\beta)^2} \right)^{\frac{1}{2}} = 1 + \frac{2\beta \tan^2 \frac{\pi}{n}}{(1+\beta)^2} + \cdots\cdots$$

Substitution of the above equation into 3.15 gives for $\beta \ll 1$

$$\gamma = \frac{\pi \tan\frac{\pi}{n}}{n} \qquad (\text{for } n \geq 3 \text{ and } \beta \ll 1) \qquad 3.17$$

or $$\gamma = \frac{\pi^2}{n^2} \qquad (\text{for } n > 20 \text{ and } \beta \ll 1)$$

Equations 3.15 or 3.17 and Figure 3.4 indicate the modes of oscillation which are possible in the loop with no contactor hysteresis. The effect of the hysteresis is best determined graphically because it is amplitude dependent. In general, by considering Figure 3.2 it can be said that the hysteresis can result

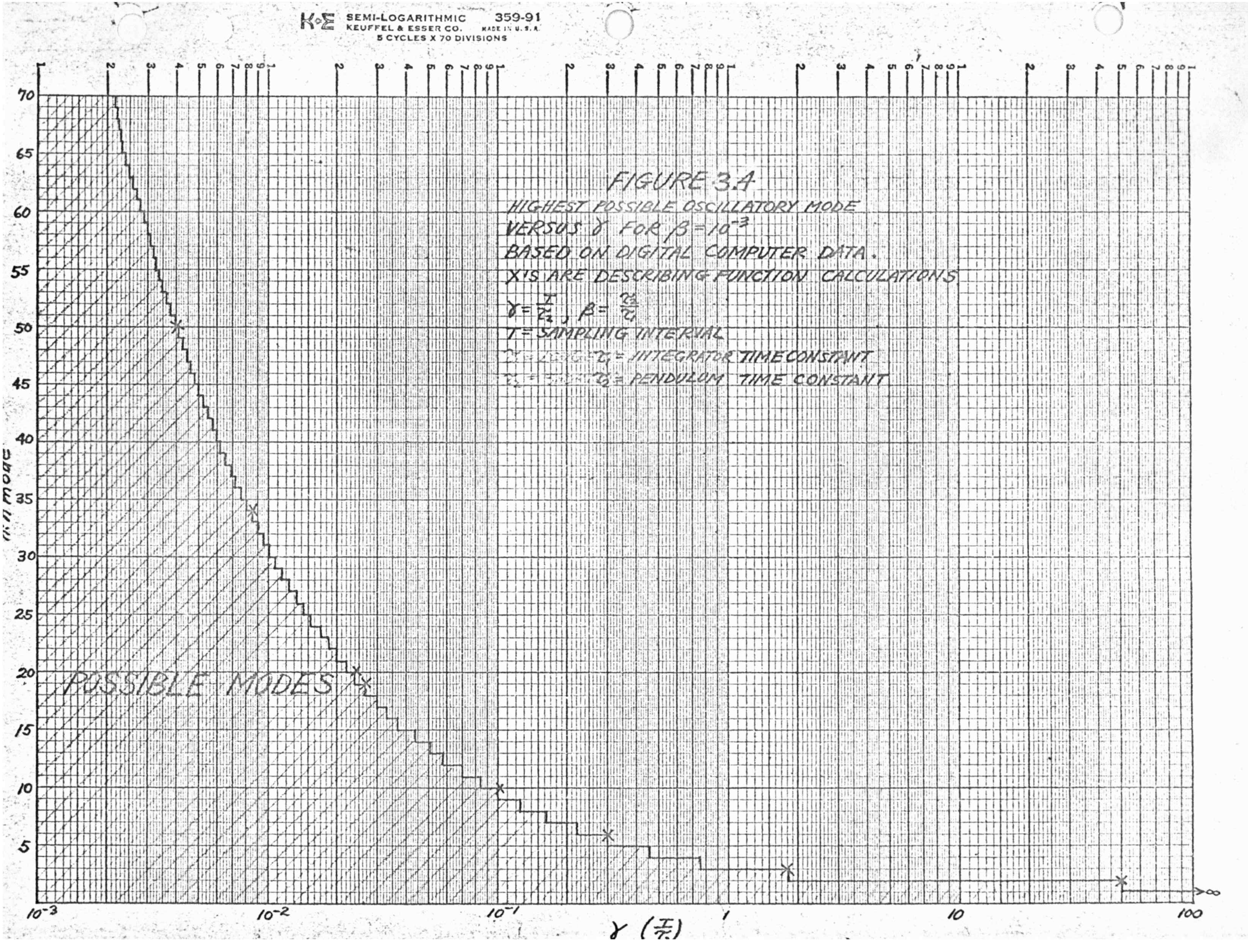
K+E SEMI-LOGARITHMIC 359-91
KEUFFEL & ESSER CO. MADE IN U.S.A.
5 CYCLES X 70 DIVISIONS
FIGURE 3.A
HIGHEST POSSIBLE OSCILLATORY MODE
VERSUS γ FOR β=10⁻³
BASED ON DIGITAL COMPUTER DATA.
X'S ARE DESCRIBING FUNCTION CALCULATIONS
γ = T/τ₂ , β = τ₂/τ₁
T = SAMPLING INTERVAL
τ₁ = INTEGRATOR TIME CONSTANT
τ₂ = PENDULUM TIME CONSTANT
POSSIBLE MODES
n mode
γ (T/τ₂)
10⁻³
10⁻²
10⁻¹
1
10
100
∞

in higher n:n modes becoming possible; however, it can also cause the lower n:n modes to become impossible.

Before attempting to extract more information about the behavior of the loop by means of the describing function analysis, an "exact" piecewise linear analysis will be made.

3.4 Piecewise Linear Analysis

Having determined the possible modes of oscillation by the describing function technique, the exact oscillatory behavior of the pendulum is obtained in this section by a piecewise linear method in order to (1) provide an analytic method for predicting the limit cycles and (2) provide further insight into the information which can be derived from the describing function.

The pendulum behaves in a linear manner with the exception of the discontinuities which occur whenever the feedback torque reverses direction. An analytic expression for the linear portion of the limit cycle can be obtained if the proper boundary conditions at the discontinuities are met in order for the oscillation to be sustained. This piecewise linear analysis gives an solution which is exact.

3.4.1. Pendulum Dynamics During Limit Cycle

With no input acceleration being applied to the pendulum, the oscillatory motion during the interval when θ is positive can be described by equation 2.3 with a = 0. Normalizing the time derivatives (i.e., $\dot{\theta} = \frac{\theta'}{T}$, $\ddot{\theta} = \frac{\theta''}{T^2}$), equation 2.3 can be written as follows:

$$\theta'' + \frac{TC}{I}\theta' + \frac{T^2K}{I}\theta = \frac{-MT^2}{I} \qquad 3.18$$

Transforming equation 3.18 from the m-domain (dimensionless time domain)

into the S-domain, where S = sT, yields the following expression where M is a constant:

$$\left(S^2 + \frac{TC}{I}S + \frac{T^2K}{I}\right)\theta_{(S)} = -\frac{MT^2}{SI} + \theta'_{n,0} + \left(S + \frac{TC}{I}\right)\theta_{n,0} \qquad 3.19$$

The left member of equation 2.4 can be factored and the equation can be written in terms of the dimensionless quantities defined in section 2.4.

$$\theta_{(S)} = \frac{-\frac{\mu\gamma}{S} + \theta'_{n,0} + \left[S + \gamma(\beta+1)\right]\theta_{n,0}}{(S+\gamma)(S+\gamma\beta)} \qquad 3.20$$

where $\gamma = \frac{T}{\tau_2}$

$\beta = \frac{\tau_2}{\tau_1}$

$\mu = \frac{TM}{C}(1+\beta)$

Transforming equation 3.20 from the S-domain back into the m-domain

$$\theta_{n,m} = \frac{1}{1-\beta}\left[\frac{-\mu}{\beta\gamma}\left(1-\beta-e^{-\beta\gamma m}+\beta e^{-\gamma m}\right) - \beta\gamma\theta_{n,0}\left(e^{-\beta\gamma m}-e^{-\gamma m}\right) - \theta'_{n,0}\left(\beta e^{-\beta\gamma m}-e^{-\gamma m}\right)\right] \qquad 3.21$$

Differentiating equation 3.21 with respect to m yields:

$$\theta'_{n,m} = \frac{1}{1-\beta}\left[-\mu\left(e^{-\beta\gamma m}-e^{-\gamma m}\right) - \beta\gamma\theta_{n,0}\left(e^{-\beta\gamma m}-e^{-\gamma m}\right) - \theta'_{n,0}\left(\beta e^{-\beta\gamma m}-e^{-\gamma m}\right)\right] \qquad 3.22$$

In order for an n:n mode of oscillation (i.e., n positive pulses followed by n negative pulses) to be self-sustaining, the following conditions must exist at the m = nth sampling instant:

$$\theta_{n,m} = -\theta_{n,0}, \quad \theta'_{n,m} = -\theta'_{n,0} \qquad 3.23$$

Substituting equations 3.23 into 3.21 and 3.22 and solving simultaneously for $\theta_{n,0}$ and $\theta'_{n,0}$ yields:

$$\theta_{n,0} = \frac{\mu}{\beta\gamma(1-\beta)}\left[\frac{1-e^{-\beta\gamma n}}{1+e^{-\beta\gamma n}} - \beta\,\frac{1-e^{-\gamma n}}{1+e^{-\gamma n}}\right] \qquad 3.24$$

$$\theta'_{n,0} = \frac{2\mu\left(e^{-\beta\gamma n}-e^{-\gamma n}\right)}{(1-\beta)(1+e^{-\gamma n})(1+e^{-\beta\gamma n})} \qquad 3.25$$

Substituting equations 3.24 and 3.25 into equation 3.21 gives the following relationship for $\theta_{n,m}$ where $0 \le m \le n$:

$$\theta_{n,m} = \frac{2\mu}{\beta\gamma(1-\beta)}\left[\frac{e^{-\beta\gamma n}}{1+e^{-\beta\gamma n}} - \frac{\beta e^{-\gamma n}}{1+e^{-\gamma n}}\right] - \frac{\mu}{\beta\gamma} \qquad 3.26$$

Equation 3.26 gives the pendulum position at the mth sampling instant after

the torquing signal changes sign in an n:n mode of limit cycle oscillation. At the particular sampling instant (m = 0) that the feedback torque changes direction, the values of $\theta_{n,o}$ and $\theta'_{n,o}$ are given by equations 3.24 and 3.25.

The exponential expressions found in equations 3.24 and 3.25 and 3.26 can be defined in terms of hyperbolic functions as follows:

$$\frac{1}{1+e^{-x}} \cdot \frac{2e^{\frac{x}{2}}}{2e^{\frac{x}{2}}} = \frac{2e^{\frac{x}{2}}}{2(e^{\frac{x}{2}}+e^{-\frac{x}{2}})} = \frac{e^{\frac{x}{2}}}{2}\,\mathrm{sech}\,\frac{x}{2}$$

$$\frac{1-e^{-x}}{1+e^{-x}} \cdot \frac{e^{\frac{x}{2}}}{e^{\frac{x}{2}}} = \frac{e^{\frac{x}{2}}-e^{-\frac{x}{2}}}{e^{\frac{x}{2}}+e^{-\frac{x}{2}}} = \tanh\frac{x}{2}$$

$$1 - e^{-\frac{x}{2}}\,\mathrm{sech}\,\frac{x}{2} = \tanh\frac{x}{2}$$

Using these relationships, equations 3.24, 3.25 and 3.26 can be written in the following manner:

$$\theta_{n,o} = \frac{\mu}{\beta\gamma(1-\beta)}\left(\tanh\frac{\beta\gamma n}{2} - \beta\tanh\frac{\gamma n}{2}\right) \qquad 3.27$$

$$\theta'_{n,o} = \frac{\mu}{(1-\beta)}\left(\tanh\frac{\beta\gamma n}{2} - \tanh\frac{\gamma n}{2}\right) \qquad 3.28$$

$$\theta_{n,m} = \frac{\mu}{\beta\gamma(1-\beta)}\left[e^{-\beta\gamma(m-\frac{n}{2})}\,\mathrm{sech}\,\frac{\beta\gamma n}{2} - \beta e^{-\gamma(m-\frac{n}{2})}\,\mathrm{sech}\,\frac{\gamma n}{2}\right] - \frac{\mu}{\beta\gamma} \qquad 3.29$$

3.42 Pendulum Dynamics During Limit Cycle, Neglecting Elastic Restraint

It is generally found that the effect of the elastic restraint on the pendulum dynamics during the limit cycle can be neglected because of the relative magnitude of the integrator time constant with respect to the limit cycle half period. At the limit cycle frequency, the pendulum behaves as if $\tau_1 \approx \infty$ (i.e., $\beta = 0$).

Letting $\beta = 0$ in equation 3.20:

$$\theta(S) = \frac{-\frac{\mu\gamma}{S} + \theta'_{n,o} + (S+\gamma)\theta_{n,o}}{S(S+\gamma)} \qquad 3.30$$

Transforming equation 3.30 from the S-domain back into the m-domain:

$$\theta_{n,m} = \theta_{n,o} + \frac{\theta'_{n,o}}{\gamma}\left(1-e^{-\gamma m}\right) - \frac{\mu}{\gamma}\left(\gamma m - 1 + e^{-\gamma m}\right) \qquad 3.31$$

Differentiating equation 3.31 with respect to m:

$$\theta'_{n,m} = \theta'_{n,o}\, e^{-\gamma m} - \mu\left(1 - e^{-\gamma m}\right) \qquad 3.32$$

At the m=nth sampling instant the following conditions are required in order for the n:n mode to be self-sustaining:

$$\theta_{n,n} = -\theta_{n,o}\,, \qquad \theta'_{n,n} = -\theta'_{n,o} \qquad 3.33$$

Substituting equations 3.33 into 3.31 and 3.32 and solving simultaneously for $\theta_{n,o}$ and $\theta'_{n,o}$ yields:

$$\theta_{n,o} = \frac{\mu}{\gamma}\left[\frac{\gamma n}{2} - \frac{1 - e^{-\gamma n}}{1 + e^{-\gamma n}}\right] \qquad 3.34$$

$$\theta'_{n,o} = \mu\,\frac{1 - e^{-\gamma n}}{1 + e^{-\gamma n}} \qquad 3.35$$

Substituting equations 3.34 and 3.35 into 3.31 gives the following expression for $\theta_{n,m}$ where $0 \leq m \leq n$.

$$\theta_{n,m} = \frac{\mu}{\gamma}\left[\frac{\gamma n}{2} - \gamma m - \frac{2e^{-\gamma m}}{1 + e^{-\gamma n}} + 1\right] \qquad 3.36$$

Equations 3.34, 3.35 and 3.36 can be written in terms of hyperbolic functions as follows:

$$\theta_{n,o} = \frac{\mu}{\gamma}\left(\frac{\gamma n}{2} - \tanh\frac{\gamma n}{2}\right) \qquad 3.37$$

$$\theta'_{n,o} = \mu \tanh\frac{\gamma n}{2} \qquad 3.38$$

$$\theta_{n,m} = \frac{\mu}{\gamma}\left[1 - \gamma\left(m - \frac{n}{2}\right) - e^{-\gamma\left(m - \frac{n}{2}\right)}\operatorname{sech}\frac{\gamma n}{2}\right] \qquad 3.39$$

3.4.3. Relating "Exact" Analysis and Describing Function Analysis

Since the integrator time constant of the experimental accelerometer is 12.5 seconds and the duration of a half-cycle for a 3:3 mode is 3T=0.0015 seconds at 2×10^3pps clock rate, the pendulum can be considered as having a perfect integrator as far as mode prediction is concerned. Thus, the simple equations of section 3.4.2 are used rather than those derived in section 3.4.1.

The steady-state pendulum outputs during the 2:2 and 3:3 modes of

oscillation are shown in Figure 3.5. The terminology $\theta_{n,m}$ refers to the pendulum angle at the mth pulse after a torque reversal during an n:n mode. The torque reverses at $\pm\theta_{n,0}$. If the hysteresis were increased to ± 1.5 seconds of arc, the 2:2 mode would no longer be self-sustaining because $\theta_{2,0}$ would occur within the hysteresis band. At that time, the hysteresis band encompasses $\theta_{4,3}$ making the 4:4 mode possible. If the hysteresis were reduced to zero; the 2:2 and 3:3 modes would still be possible, in addition to the 1:1. This is substantiated by the describing function curve of Figure 3.3. The locus of $\frac{-1}{G_D}$ for zero hysteresis lies along the -180 line. The $\phi_{G(j\omega)}$ for all three of these modes intersect -180°.

Having the "exact" pendulum response in Figure 3.5, some additional moding information can be obtained from the describing function in Figure 3.3 by relating the two curves. The amplitude of an n:n mode of oscillation can be obtained by evaluating equation 3.8 at the frequency of the n:n mode, $\omega = \frac{\pi}{nT}$.

$$|\theta| = \frac{\mu B \delta}{\left[1 + \left(\frac{\pi}{B\delta n}\right)^2\right]^{\frac{1}{2}} \left[1 + \left(\frac{\pi}{\delta n}\right)^2\right]^{\frac{1}{2}}} \qquad 3.40$$

Without a sampler in the loop, the system, according to Figure 3.3 would limit cycle at the frequency where $\phi_{-\frac{1}{G_D}}$ intersects ϕ_{pendulum}, $\omega = 3.65 \times 10^3$ radians/second. For this situation, $\pm\theta_{n,0}$ would equal $\pm\Delta\theta$ (i.e., $\pm$ 1 second of arc.) The inclusion of a sampler with a clock rate of 2×10^3 pps causes the system to limit cycles at 3.14×10^3 rad./sec. (2:2 mode) or 2.1×10^{-3} rad./sec. (3:3 mode). The sampler contributes a phase shift of $\alpha_{2:2}$ and $\alpha_{3:3}$ for the 2:2 and 3:3 modes, respectively.

The crossing of the zero reference axis in Figure 3.5 by the pendulum cannot be detected until the pendulum leaves the hysteresis band. The

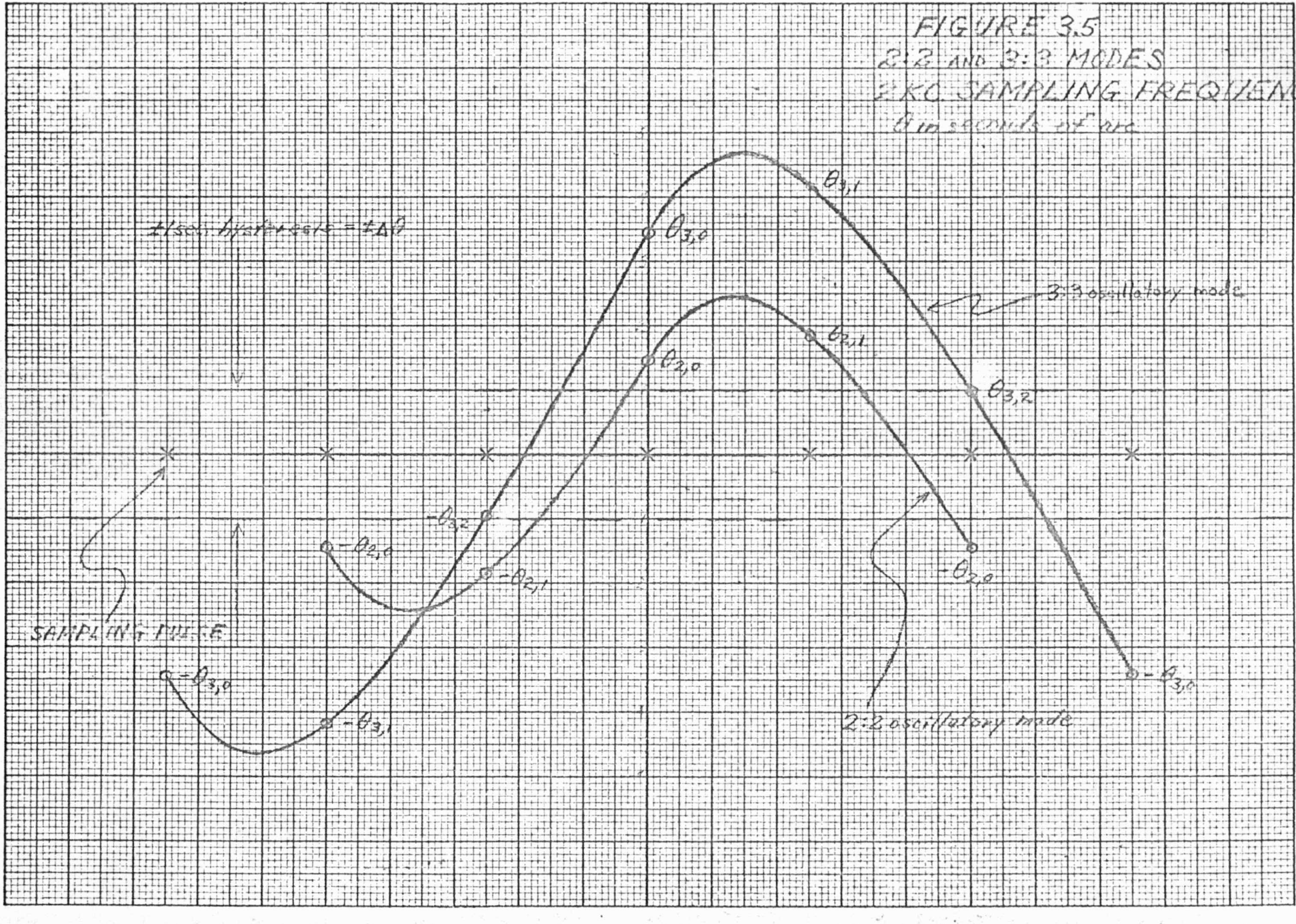

effective phase shift is defined by the describing function as $\sin^{-1}\frac{\Delta\theta}{|\theta|}$.

According to Figure 3.3,

$$\delta_{n:n} - \alpha_{n:n} = \sin^{-1}\frac{\Delta\theta}{|\theta|_{n:n}} \qquad 3.41$$

Since the torque feedback signal is not switched until $\theta_{n,o}$, it is evident from equation 3.41, Figure 3.3 and Figure 3.5 that a similar expression involving $\theta_{n,o}$ can now be written.

$$\delta_{n:n} = \sin^{-1}\frac{\theta_{n,o}}{|\theta|_{n:n}}$$

$$\text{or} \quad \theta_{n,o} = |\theta|_{n:n}\sin\delta_{n:n} \qquad 3.42$$

Similarly,

$$\theta_{n,n-1} = |\theta|_{n:n}\sin\left(\frac{\pi}{n} - \delta_{n:n}\right) \qquad 3.43$$

Thus, the pendulum angle at the two critical sampling instants can be determined semi-graphically. This does not exhause the information obtainable from the describing function analysis. References to Figure 3.3 will be made in other sections of this report. The accuracy of the describing function depends on the particular system parameters and operating conditions. In the case under investigation, the higher harmonics contribute very little phase shift and distortion to the fundamental sinusoid. The describing function analysis and the piecewise linearization analysis agree very well.

3.5 Analytic Mode Prediction

A convenient semigraphical method of predicting the oscillatory modes is afforded by the describing function. An "exact" analytic expression for the possible n:n modes can be obtained from the equations used in the piecewise linear analysis.

Without a sampler in the loop, $\theta_{n,o} = \Delta\theta$ since the torque feedback reverses polarity at the instant the pendulum leaves the hysteresis band.

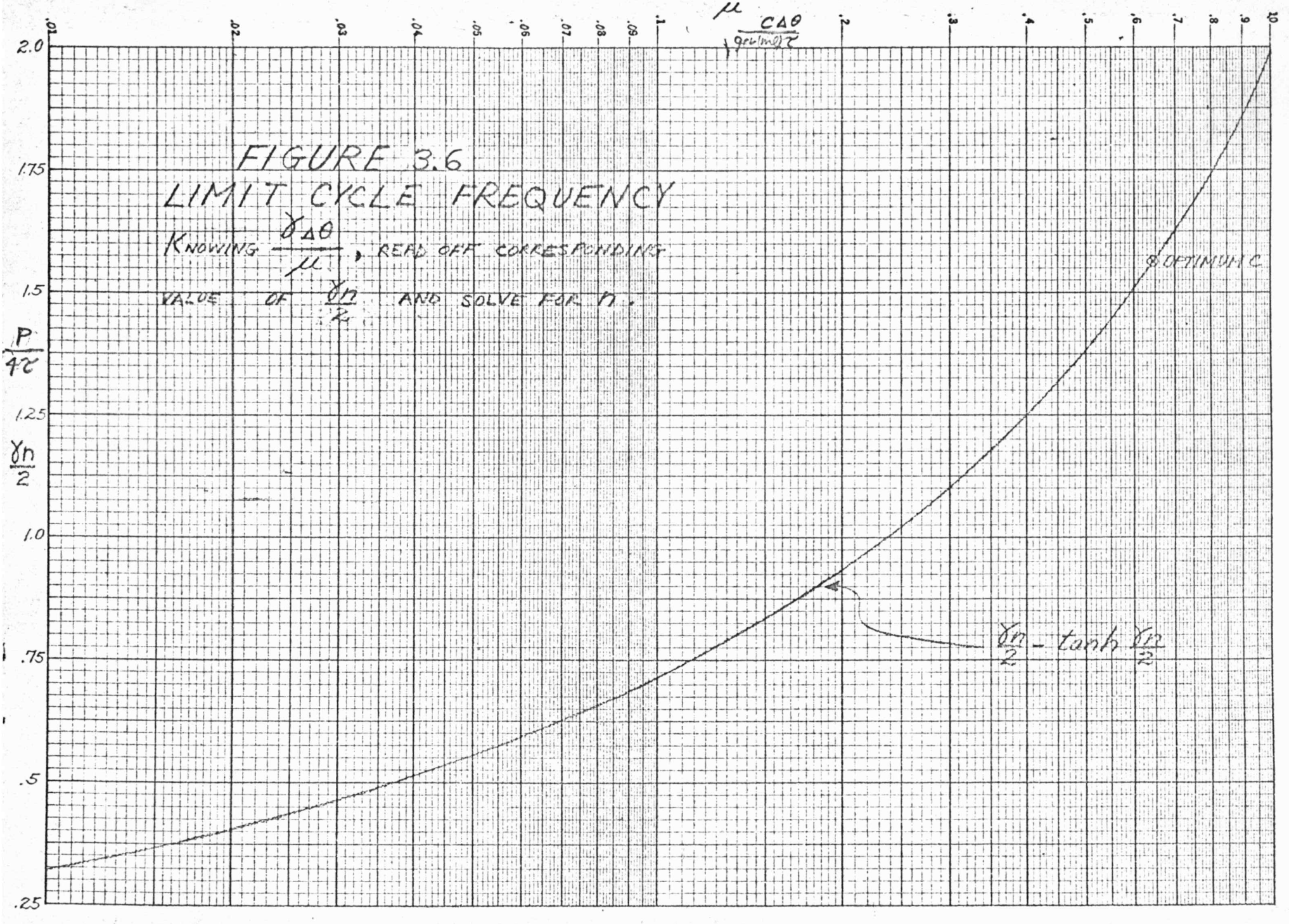

Letting $\theta_{n,o} = \Delta\theta$ in equation 3.37 yields

$$\Delta\theta = \frac{\mu}{\gamma}\left(\frac{\gamma n}{2} - \tanh\frac{\gamma n}{2}\right)$$

or

$$\frac{\gamma\Delta\theta}{\mu} = \frac{\gamma n}{2} - \tanh\frac{\gamma n}{2} \qquad 3.44$$

For small values of $\frac{\gamma\Delta\theta}{\mu}$, the tanh can be expressed as the first two terms of its series expansion.

$$\tanh\frac{\gamma n}{2} = \frac{\gamma n}{2} - \frac{1}{3}\left(\frac{\gamma n}{2}\right)^3 + \ldots\ldots \qquad 3.45$$

Substituting equation 3.45 into 3.44,

$$\frac{\gamma\Delta\theta}{\mu} = \frac{1}{3}\left(\frac{\gamma n}{2}\right)^3$$

or

$$n = \sqrt[3]{\frac{24\Delta\theta}{\mu\gamma^2}} \qquad \text{for } \frac{\gamma\Delta\theta}{\mu} < .01 \qquad 3.46$$

The n evaluated in equation 3.46 will most likely be a non-integer number. The possible n:n modes, with a sampler in the loop, will then be such that the values of n are the next two higher integers above the value of n given by equation 3.46.

For large values of $\frac{\gamma\Delta\theta}{\mu}$, $\tanh\frac{\gamma n}{2} \approx 1$ and equation 3.44 can be written as

$$\frac{\gamma\Delta\theta}{\mu} = \frac{\gamma n}{2} - 1$$

or

$$n = \frac{2}{\gamma}\left(1 + \frac{\gamma\Delta\theta}{\mu}\right) \qquad \text{for } \frac{\gamma\Delta\theta}{\mu} > 1 \qquad 3.47$$

If $.01 < \frac{\gamma\Delta\theta}{\mu} < 1$, the curve in Figure 3.6 is used to determine n. Knowing $\frac{\gamma\Delta\theta}{\mu}$, determine $\frac{\gamma n}{2}$ from the curve and solve for n. In general, depending on the magnitude of $\frac{\gamma\Delta\theta}{\mu}$, n is determined with use of equations 3.46, equation 3.47 or Figure 3.6. This value of n would correspond to the limit cycle frequency, $\omega = \frac{\pi}{nT}$, which would exist in the loop which has no sampler. The presence of the sampler makes several n:n modes possible. These n:n modes would be such that values of n are the next two higher integers above the non-

integer value of n determined for the non-sampled case.

There is a possibility that three, rather than two, n:n modes are possible. For example, it is evident from Figure 3.2 that a small increase in $\pm \Delta\theta$ from its value of ± 1 second of arc would cause $\frac{-1}{G_D}$ to intersect the possible effective sampler phase shift of the 4:4, 3:3 and 2:2 modes. This condition occurs if the determined value of n for an unsampled loop is just slightly less than an integer.

CHAPTER IV

System Response to Acceleration Inputs

Graphical and analytic methods of predicting the possible oscillatory modes of a sample-data contactor feedback control system were presented in Chapter III for the case with no input being applied. The effect of contactor hysteresis was also considered. In this chapter, the response of this nonlinear system to a small input will be investigated. The principle of superposition does not, in general, apply to a nonlinear system (i.e., the response of the system to one input cannot be ordinarily determined from the response of the system to some other input.) This is the reason why it is usually difficult to obtain a general solution of the dynamic response of a nonlinear system. However, for small inputs, the analysis of this chapter provides a simple, but accurate, description of the dynamic behavior of the system. This technique involves the superposition of the linear open-loop response of the pendulum upon the steady-state oscillation of the closed-loop nonlinear system. The results of the analog computer simulation substantiate the validity of using such a technique.

4.1 Mode Switching Angle

The behavior of the pendulum for the 2:2 and 3:3 modes are shown in Figure 3.5. The existence of these two modes was determined by obtaining the initial conditions at the beginning of each torque half cycle required to make the limit cycle period equal to $2nT$. In addition, it was required that $\theta_{n,o}$ be larger than $+\Delta\theta$ and that the pendulum angle be more positive than $-\Delta\theta$ at all the sampling instants between $\theta_{n,o}$ and $\theta_{n,n-1}$, inclusively.

In order for the limit cycle to continue indefinitely, $\theta_{n,n}$ must equal

$-\theta_{n\rho}$. For the moding to continue only from one torque cycle to another, $\theta_{n,n}$ need not necessarily equal $-\theta_{n,o}$. All that is required is that no change in the polarity of the pendulum angle be detected at any sampling instant until the nth sampling instant. For a small amplitude, slowly varying acceleration input, the wave shapes in Figure 3.5 can be considered as moving slowly up and down. The 2:2 wave can move upward until $-\theta_{2,o}$ enters the hysteresis band and the torque does not reverse until the arrival of the next pulse as the system enters the 3:3 mode. Likewise, the 2:2 wave could move downward until $\theta_{2,o}$ enters the hysteresis band. The mode switching angle for the 2:2 mode is therefore $\pm\theta_{2,o}$.

The 3:3 wave can move upward until $-\theta_{3,2}$ passes through the hysteresis band and the torque reverses on the second sampling pulse of the torque half cycle rather than the third pulse as the system enters the 2:2 mode. Similarly, the 3:3 wave can move downward until $\theta_{3,2}$ passes through the hysteresis band. Thus $\pm\theta_{3,2}$ is the mode switching angle for the 3:3 mode.

The mode switching angle depends on the wave shape of the particular n:n mode and the size of the hysteresis angle. For a rapidly changing acceleration input, the torque reversal could come at any sampling instant. However, with a small amplitude, slowly varying input, the mode switching angle will be

$$\begin{aligned} &\pm\theta_{n,o} \quad \text{if } |\theta_{n,o}-(+\Delta\theta)| < |(-\Delta\theta)-\theta_{n,n-1}| \\ &\pm\theta_{n,n-1} \quad \text{if } |\theta_{n,o}-(+\Delta\theta)| > |(-\Delta\theta)-\theta_{n,n-1}| \end{aligned} \qquad 4.1$$

According to the describing function in Figure 3.3, the mode switching angle is

$$\begin{aligned} &|\theta|_{n:n}\sin\delta_{n:n} \quad \text{if } \alpha_{n:n} < \lambda_{n:n} \\ &|\theta|_{n:n}\sin\left(\tfrac{\pi}{n}-\delta_{n:n}\right) \quad \text{if } \alpha_{n:n} > \lambda_{n:n} \end{aligned}$$

4.2 Open Loop Response of Pendulum to Step Input

For small inputs, the nonlinear system can be considered as operating in a limit cycle with the input simply affecting the average value of the oscillating pendulum. The approach which will be used in obtaining the response of the system to an applied acceleration will consist of determining when the average value of the limit cycle reacts to the step input such that it causes a change from one of the possible modes to the other. The average value of the limit cycle moves away from its reference position when an acceleration is applied until the mode switching angle reaches the hysteresis band and the mode changes.

The reaction of the average value of the pendulum limit cycle to the acceleration input can be obtained from the open loop response of the pendulum to a step input. The response, according to equation 2.4 is

$$\theta_{(t)} = \frac{P_a}{K}\left[1 + \frac{\frac{\tau_2}{\tau_1}e^{-t/\tau_2} - e^{-t/\tau_1}}{1 - \frac{\tau_2}{\tau_1}}\right] \qquad 4.2$$

After the transient portion has decayed exponentially to a negligible value, the pendulum approaches the steady-state value,

$$\theta_{ss} = \frac{P_a}{K} \qquad 4.3$$

With no elastic restraint, K', in the pendulum; the response according to equation 2.4 is

$$\theta_{(t)} = \frac{P_a}{C}\left(t - \tau_2 + \tau_2 e^{-t/\tau_2}\right) \qquad 4.4$$

The steady-state response to the step input is therefore a ramp when K = 0.

4.3 System Response to a Step Input

Assume no elastic restraint for the present, the average value of the pendulum in the 2:2 mode moves upward in Figure 3.5 due to a small step input of acceleration. Eventually, during one of the positive half cycles, $-\theta_{2,o}$ will occur within the hysteresis band and the 2:2 mode will switch to a 3:3 mode.

Since the mode switch occurred at the beginning of the torque cycle, the up-and-down counter will produce no net change. With the step input still applied to the pendulum, the average value of pendulum limit cycle, now in the 3:3 mode, will continue to move upward.

Eventually, during a negative half cycle of the pendulum, the 3:3 wave in Figure 3.5 will have moved upward such that $-\theta_{3,2}$ occurs outside the hysteresis band and the torque reverses immediately as the system goes back into the 2:2 mode. During this particular torque cycle, the counter will have counted up 3, counted down 2 and therefore gives a net output of one $=\Delta V$ pulse. If the step input persists, the system will continue to change between the 2:2 and 3:3 modes, giving a net output every time the mode switches from a 3:3 to a 2:2 mode.

The application of a acceleration step input of the opposite polarity will cause the waveforms in Figure 3.5 to move downward. The modes change again at the mode switching angles described in section 4.1. The only difference with the negative step input, is that counter produces a net output as the mode switches from a 2:2 to a 3:3 mode.

The behavior of the system in response to an acceleration step input can be considered in the following manner. Since there are generally only two modes possible, the system can only switch between the two modes. If the system is in a 2:2 mode and a positive acceleration is applied, eventually a $+\Delta$ V pulse will be required. The occurrence of a 2:3 cycle after a number of 2:2 cycles with a positive acceleration being applied would be an impossibility since this would result in a net $-\Delta V$ pulse. What actually happens if that system "slips" into the 3:3 moding by producing a 3:3 cycle after a number of 2:2 cycles. No net output of the counter is produced during this change of modes because the change

occurred at the end of a negative half cycle of the pendulum oscillation which is the time when the contents of the counter are examined. The system continues in the 3:3 mode under the influence of the step input. Eventually, a 3:2 cycle occurs which is detected by the up-and-down counter as a net $+\Delta V$ pulse. With the step input remaining applied to the pendulum, the system will continue to change repeated between the two modes with the incremental velocity information becoming available at a rate this quantized data best indicates the time integral of acceleration. The response of the simulated accelerometer to acceleration step inputs of various amplitudes are shown in the Appendix.

This heuristic development of a description of the system response to a step input may also be presented with the use of the phase-plane. The phase plane trajectories for the 2:2 and 3:3 modes are shown in Figure 4.1. The hysteresis band and the sampling instants are also shown on the plot. A plot of the 4:4 and 1:1 trajectories would show that these modes are impossible because of the relative location of $\pm\theta_{4,3}$, $\pm\theta_{1,0}$ and the hysteresis band.

With no elastic restraint in the pendulum, the trajectories move to the right or left under the influence of an acceleration step input. This lateral motion of the trajectory continues until $\theta_{n,o}$ enters the hysteresis band or else $\theta_{n,n-1}$ passes through the hysteresis band and the mode switches. This mode switching continues as the incremental velocity information is generated. The horizontal bars through sampling points indicate the possible lateral displacements of these sampling points that can exist. The discussion of the system behavior in this section can be followed in conjunction with the trajectories of Figure 4.1. A typical trajectory of the simulated accelerometer is shown in Figure A.2 of the Appendix.

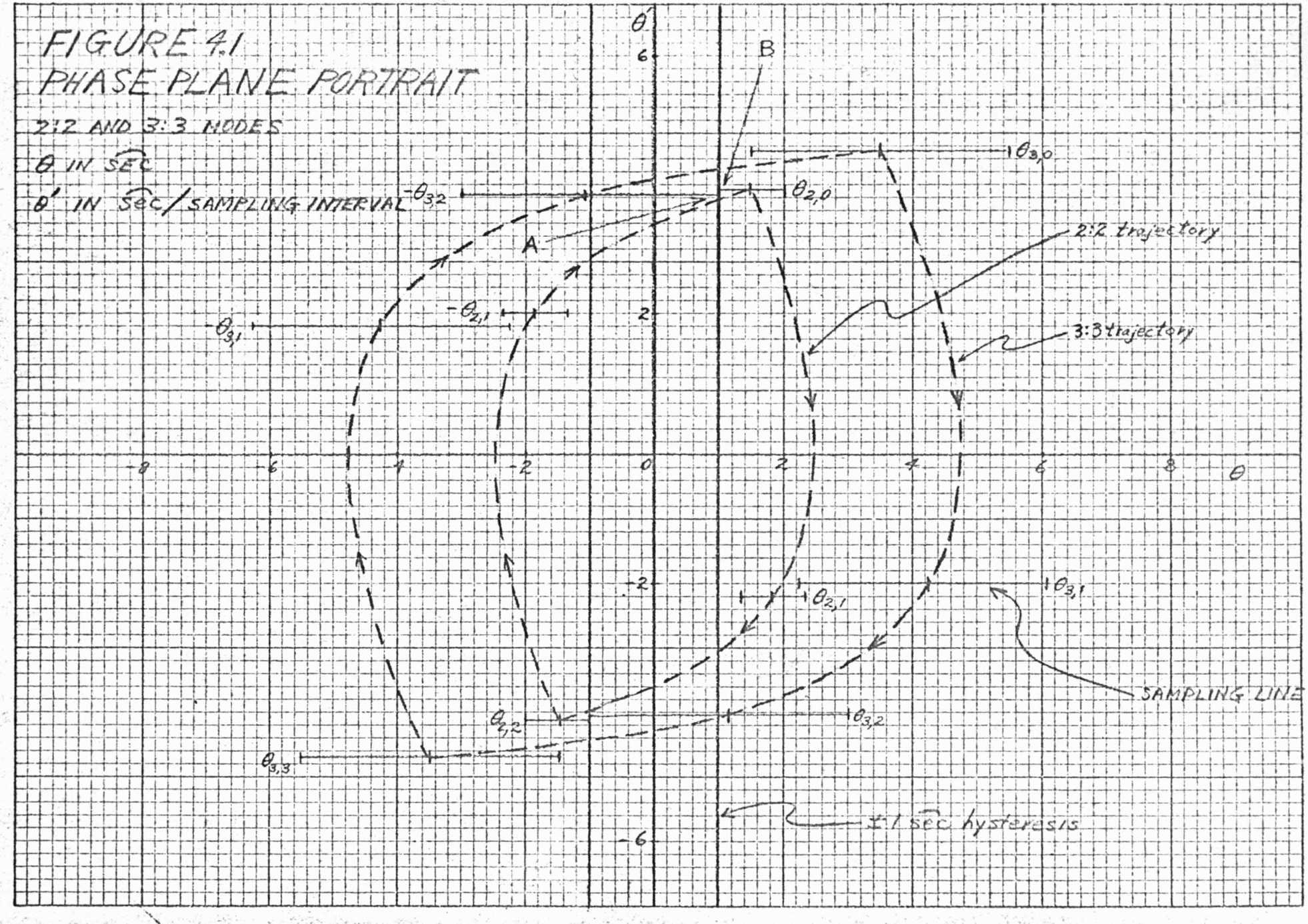

This description of the system response to a small step input of acceleration was substantiated by the analog computer simulation. The system response to large amplitude, rapidly-varying inputs is much more difficult to ascertain because the greater number of possible modes and mode switching angles makes a general theory of mode response impossible. However, an extensive computer simulation can provide some general information on responses to large inputs. This would be the suggested method of investigating large inputs.

4.4 Accelerometer Deadzone Due to Elastic Restraint

The steady state response of the average value of the pendulum angle to an acceleration step input is given by equation 4.3 and repeated below where $K = Pg + K'$.

$$\theta_{ss} = \frac{Pa}{K} = \frac{Pa}{Pg + K'} = \frac{a}{g}\left(\frac{1}{1 + \frac{K'}{Pg}}\right)$$

It was shown in section 4.1 that mode switching occurs whenever the average value of the limit cycle exceeds $\pm|\theta_{n,o} - (+\Delta\theta)|$ or $\pm|(-\Delta\theta) - \theta_{n,n-1}|$, whichever is smaller. Therefore, if the average value of the limit cycle required for mode switching is not exceeded as the pendulum angle approaches θ_{ss}, a sensible output of the accelerometer will not be produced. (See Figures A.15b and A.16 in the Appendix). Setting the smaller of $\pm\left|\theta_{n,o} - (+\Delta\theta)\right|$ or $\pm\left|(-\Delta\theta) - \theta_{n,n-1}\right|$ equal to θ_{ss} gives the bounds of the deadzone for that particular n:n mode.

$$\text{DEADZONE}_{n:n} = \pm|\theta_{n,o} - (+\Delta\theta)|\left(1 + \frac{K'}{Pg}\right) g's \quad \text{if } |\theta_{n,o} - (+\Delta\theta)| < |(-\Delta\theta) - \theta_{n,n-1}|$$

$$\text{or } \pm|(-\Delta\theta) - \theta_{n,n-1}|\left(1 + \frac{K'}{Pg}\right) g's \quad \text{if } |\theta_{n,o} - (+\Delta\theta)| > |(-\Delta\theta) - \theta_{n,n-1}| \qquad 4.6$$

Repeated switching between the two possible modes is required in order to obtain the proper output due to a step input. Furthermore, the deadzones for the two modes are generally not the same such that an acceleration input may be outside the deadzone for one of the modes, but within the deadzone

for the other. Thus, the actual accelerometer deadzone is the larger of the two deadzones for the possible n:n modes.

The deadzones for the possible modes, given by equations 4.6, were plotted versus the hysteresis angle in Figure 4.2. The actual accelerometer deadzone at any value of hysteresis is the larger of the two mode deadzones. Note that there are values of hysteresis which will allow three different modes to be possible. It is apparent from Figure 4.2 that the minimum accelerometer deadzones occur when the deadzones for the two possible modes are equal.

The accelerometer deadzone can also be determined from the describing function analysis. According to section 3.4.3

$$\left|\theta_{n,o}-(+\Delta\theta)\right| = |\theta|_{n:n}\left[\sin\delta_{n:n} - \sin(\delta_{n:n}-\alpha_{n:n})\right]$$
$$\left|(-\Delta\theta)-\theta_{n,n-1}\right| = |\theta|_{n:n}\left[\sin(\delta_{n:n}-\alpha_{n:n}) + \sin(\tfrac{\pi}{n}-\delta_{n:n})\right] \qquad 4.7$$

The deadzone for a particular n:n mode can be obtained with use of Figure 4.2

$$\text{Deadzone}_{n:n} = \pm|\theta|_{n:n}\left[\sin\delta_{n:n} - \sin(\delta_{n:n}-\alpha_{n:n})\right]\left(1+\tfrac{K'}{P_g}\right)g's \quad \text{if } \alpha_{n:n}<\lambda_{n:n}$$
$$\text{or} \quad \pm|\theta|_{n:n}\left[\sin(\delta_{n:n}-\alpha_{n:n}) + \sin(\tfrac{\pi}{n}-\delta_{n:n})\right]\left(1+\tfrac{K'}{P_g}\right)g's \quad \text{if } \alpha_{n:n}>\lambda_{n:n} \qquad 4.8$$

Again, the actual accelerometer deadzone is the larger of the two deadzones for the possible n:n modes.

Consider the experimental accelerometer with the parameters given in equation 3.9. With the hysteresis set at $\pm$ 1 second of arc, it is evident from Figure 3.3 that

$$\alpha_{2:2} < \lambda_{2:2}$$
$$\alpha_{3:3} > \lambda_{3:3}$$

Therefore, the deadzones for the two modes are

$$\text{Deadzone}_{2:2} = \pm|\theta|_{2:2}\left[\sin\delta_{2:2} - \sin(\delta_{2:2}-\alpha_{2:2})\right]\left(1+\tfrac{K'}{P_g}\right)g's$$
$$\text{Deadzone}_{3:3} = \pm|\theta|_{3:3}\left[\sin(\delta_{3:3}-\alpha_{3:3}) + \sin(\tfrac{\pi}{3}-\delta_{3:3})\right]\left(1+\tfrac{K'}{P_g}\right)g's$$

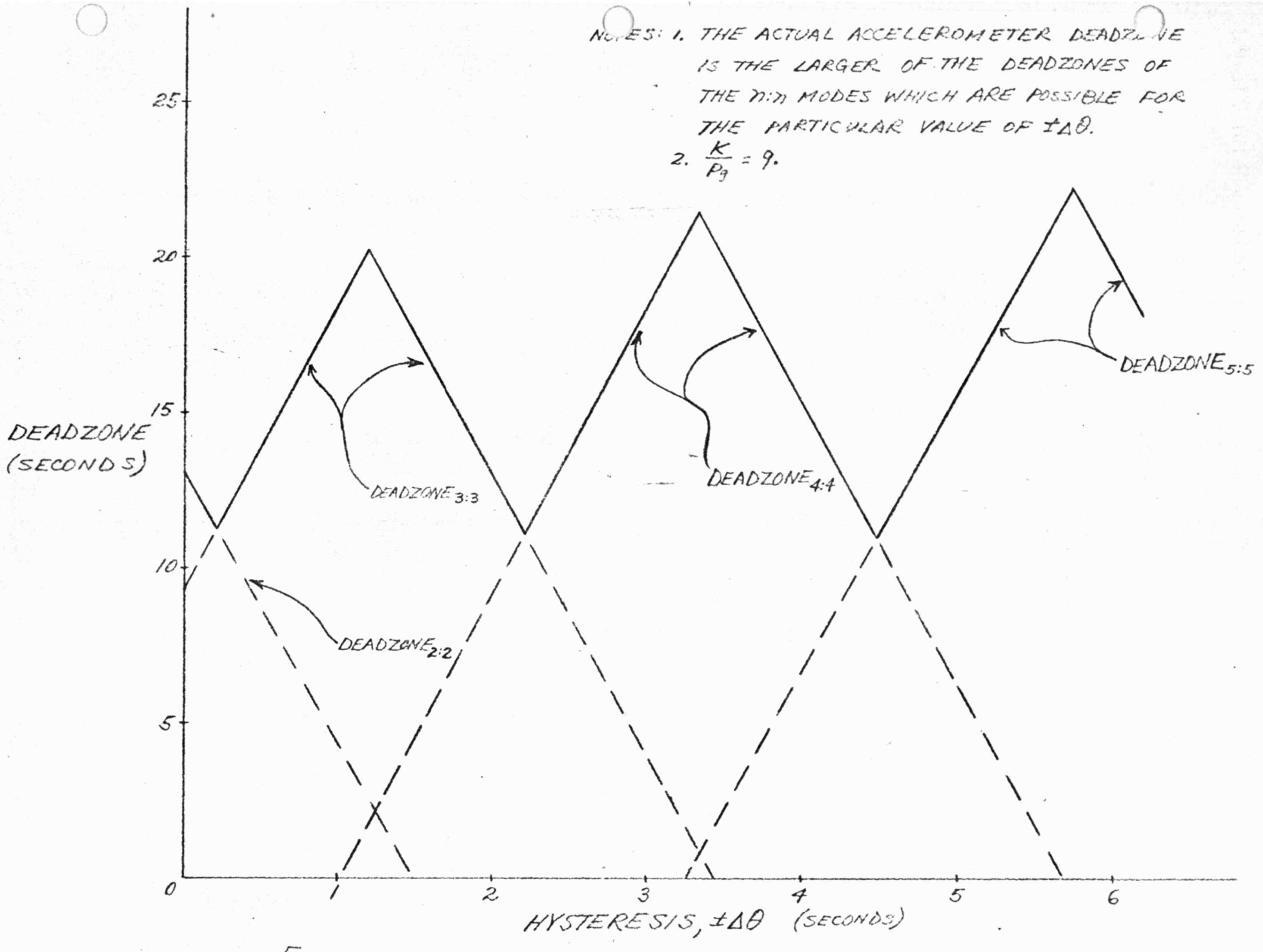

Fig 4.2 DEADZONE VS. HYSTERESIS ANGLE

Since $|\theta|_{2:2} = 2.5$ seconds of arc and $|\theta|_{3:3} = 4.7$ seconds of arc according to Figure 3.4, the deadzones for $\frac{K'}{Pg} = 8$ are

$$\text{Deadzone}_{2:2} = \pm 2.25 \times 10^{-5} g's$$

$$\text{Deadzone}_{3:3} = \pm 9 \times 10^{-5} g's$$

Thus the actual accelerometer deadzone is the larger of the two deadzones; namely, $\pm 9 \times 10^{-5} g's$.

Even if the step input is slightly larger than the value of the deadzone given by equations 4.6 or 4.8, the pendulum would tend to approach its steady state value exponentially rather than linearly as it would in the absence of elastic restraint. Although this would not result in a complete loss of information, as is the case within the deadzone, it would result in an undesirable partial loss of information due to a time lag in the production of a sensible accelerometer output. (See Figure A.17 in the Appendix). In other words, the presence of elastic restraint causes the accelerometer sensitivity to be nonlinear immediately outside the deadzone in addition to the definite nonlinearity within the deadzone.

4.5 Mode Switching Without Producing Output

The repeated switching between the 2:2 and 3:3 modes is associated with an acceleration input, according to the discussion in the previous section. However, there is a very small region of limit cycle conditions which can result in the system switching repeatedly between the 2:2 and 3:3 modes without an acceleration input being applied.

Consider the situation where the system is in a 3:3 mode and a small acceleration is applied so that the 3:3 trajectory in Figure 4.1 moves to the right. When $-\theta_{3,2}$ reaches the $-\Delta\theta$ at point A, the system switches from the

The time constant of the torquer should be small or else it must be considered during the calculation of the pendulum dynamics.

5.4 Clock Frequency

The minimum clock frequency should be such that T is equal to, or less than, the feedback acceleration $(\frac{M}{K})$ divided by the desired increment of velocity, in order to obtain the specified resolution in the velocity indication.

$$T \leq \frac{M}{K\Delta V} \qquad 5.3$$

The accuracy of the clock frequency must be better than the accuracy specification for the system and the width of the clock pulse should be very narrow in order to reduce the uncertainty in the time that switching occurs.

5.5 Elastic Restraint

It is desirable that there be no elastic restraint in the pendulum because of the deadzone and nonlinearity it produces. The deadzone effect can be seen by comparing Figure A.15b and A.16 in the Appendix. The elimination of the deadzone removes the uncertainty of the pendulum position in the vicinity of its reference position. The nonlinearity refers to the scale factor of the accelerometer being affected by the time delay in producing a ΔV output. This is due to the fact that the average value of the pendulum "limit cycle" moves away from its reference position in an exponential manner rather than linearly. This time delay increases as the input decreases; such that it approaches infinity as the input reduces to the deadzone level. This nonlinear effect is shown in Figure A.17 of the Appendix.

5.6 Pendulum Time Constant

In order for the accelerometer system to operate in an optimum fashion,

3:3 into the 2:2. Assume that the step input is removed shortly thereafter. Since $-\theta_{3,2}$ is slightly less than the value of $\theta_{2,0}$ required for a 2:2 mode to be self-sustaining, the pendulum will tend to overshoot to the left during the first 2:2 cycle. The 2:2 mode will tend to complete its cycle to the left of point B, which is clearly impossible because of the hystersis band. Thus, the system will return to the 3:3 mode. Since $-\theta_{3,2}$ for this first cycle is slightly larger than the normal value of $-\theta_{3,2}$, the trajectory will overshoot slightly to the right during this initial 3:3, so that it returns to the 2:2 at the end of this single 3:3 cycle.

The possibility of such a mode existing indefinitely was proven by considering a periodic mode consisting of ten pulses have a +3, -2, +2, -3 sequence. Using the piecewise linear equations derived in section 3.4.2 to describe the behavior of the pendulum between torque reversals, a set of initial conditions were obtained so that θ and θ' at the first and tenth sampling instants were equal but of opposite sign. In addition, the requirements for the sense of the pendulum angle at the intermediate sampling instants were met making it possible for this particular mode to be self-sustaining indefinitely.

Since this particular type of limit cycle appears to be relatively unstable in comparison with the 2:2 and 3:3 modes, it was difficult to have the analog computer simulation of this moding to persist more than about five cycles. (See Figure A.18 in the Appendix).

CHAPTER V

Accelerometer System Synthesis

5.1 General

During the course of analyzing the pulse torqued accelerometer, the effects of the system parameters upon the behavior of the nonlinear system were uncovered. Knowing the performance characteristics which are desirable in the system, it is appropriate at the conclusion of the analysis to provide a guide which may be used for the selection of the system parameters in the synthesis of an accelerometer system.

It is not the purpose of this chapter to become concerned with the problems associated with the physical realization of such a system; rather to present a mathematical guide to the development of an accelerometer which meet the specifications established by a proposed application.

5.2 Pendulosity

It is desirable to keep the pendulosity small in the pendulum since it does have an effect on the size and weight of the instrument. The product of the pendulosity and the minimum acceleration to be measured should be greater than the torque uncertainty in the system in order to insure proper detection of an input.

$$Pa_{min.} > M_{uncertainty} \qquad 5.1$$

5.3 Torque Generator

The minimum torquing level, $\pm$ M, must be greater than the product of the pendulosity and maximum acceleration to be measured in order to provide the specified range.

$$M > Pa_{max.} \qquad 5.2$$

the "limit cycle" amplitude should be kept as small as possible in order to reduce the instantaneous error in the velocity indication. This corresponds to having a "tight"loop in a linear control system. The frequency of the "limit cycle" should also be high in order that the change in velocity can be detected in the shortest possible time. In this regard, the pendulum time constant $(\frac{I}{C})$ should be as small as is practical.

Efforts should be made to keep the inertia low. Therefore, it would be desirable that the torque and signal generators require very little material to be located on the float. The damping should be high in order to reduce the angle through which the pendulum travels. Yet it should be low so that the average value of the "limit cycle" moves away from its reference position at a high angular rate in order to detect a change in velocity in the shortest time possible. Thus, there appears to be an optimum value of damping for which the "limit cycle" frequency is maximum. This optimum value of damping will now be determined from the describing function analysis for the system which has no sampler.

According to the describing function analysis, the system "limit cycles" when

$$\phi_{\text{pendulum}} = \phi_{-\frac{1}{G_D}}$$

or

$$-\frac{\pi}{2} + \tan^{-1}\omega\tau_2 = -\pi + \sin^{-1}\frac{\Delta\theta}{|\theta|} \qquad 5.4$$

Rewriting equation 5.4

$$\tan^{-1}\omega\tau_2 = -\frac{\pi}{2} + \sin^{-1}\frac{\Delta\theta}{|\theta|} \qquad 5.5$$

Taking the cosine of both sides of equation 5.5

$$\cos\left(\tan^{-1}\omega\tau_2\right) = \cos\left(\sin^{-1}\frac{\Delta\theta}{|\theta|} - \frac{\pi}{2}\right) = \frac{\Delta\theta}{|\theta|} \qquad 5.6$$

Knowing that $\tan^{-1}-\omega\tau_2$ is the phase angle of $\frac{1}{1+j\omega\tau_2}$, the following right triangle can be constructed:

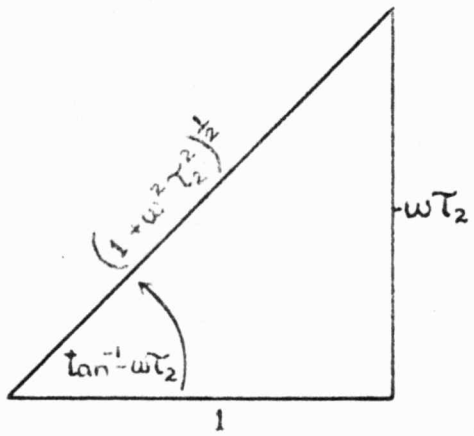

From the right triangle it is evident that

$$\cos\left(\tan^{-1}-\omega\tau_2\right) = \frac{1}{\left(1+\omega^2\tau_2^2\right)^{\frac{1}{2}}} \qquad 5.7$$

Neglecting the integrator time constant, the amplitude of the pendulum limit cycle can be obtained from the frequency response of the pendulum to the fundemental component of the square wave driving it. Thus

$$|\theta| = \frac{\frac{4}{\pi}\frac{M}{C}}{\omega\left(1+\omega^2\tau_2^2\right)^{\frac{1}{2}}} \qquad 5.8$$

Substituting equations 5.7 and 5.8 into 5.6 gives

$$\frac{1}{\left(1+\omega^2\tau_2^2\right)^{\frac{1}{2}}} = \frac{\pi C\Delta\theta}{4M}\omega\left(1+\omega^2\tau_2^2\right)^{\frac{1}{2}}$$

Since $\tau_2 = \frac{1}{C}$ the above equation can be written as:

$$\frac{4MC}{\pi\Delta\theta} = C^2\omega + \omega^3 I^2 \qquad 5.9$$

According to equation 5.9, the frequency of oscillation can be increased by increasing M and decreasing $\Delta\theta$ and I. However, once these three quantities are fixed, the value of C which maximizes ω can be determined as follows:

Take the partial derivative of ω with respect to C in equation 5.9

$$\frac{4M}{\pi\Delta\theta} = 2C\omega + C^2\frac{\partial\omega}{\partial C} + 3\omega^2 I^2\frac{\partial\omega}{\partial C}$$

Set $\frac{\partial \omega}{\partial C}$ equal to zero and solve for $\omega_{max.}$ which exists for optimum damping.

$$\omega_{max.} = \frac{2M}{\pi C \Delta\theta} \qquad 5.10$$

Substituting equation 5.10 into 5.9 and solving for optimum C yields:

$$C = \sqrt{\frac{2MI}{\pi \Delta\theta}} \qquad 5.11$$

Solving for $\omega\tau_2$ using equations 5.10 and 5.11

$$\omega\tau_2 = 1$$

or

$$\omega = \frac{1}{\tau_2} \qquad 5.12$$

When the pendulum time constant contributes 45° of phase shift in accordance with equation 5.12, the hysteresis describing function also contributes 45° or i.e.,

$$\phi_{-\frac{1}{G_D}} = \sin^{-1}\frac{\Delta\theta}{|\theta|} = 45°$$

or

$$\Delta\theta = .707|\theta|$$

Equation 5.12 gives the relationship between the amplitude of the "limit cycle" and the torque switching angle which gives the maximum limit cycle frequency. A plot of ω versus C would show the curve to be quite flat around the optimum value of C.

CHAPTER VI

Conclusions and Recommendations

This report has been concerned with the analysis of a pulse torqued accelerometer with zero and small inputs. The describing function technique was used extensively to determine the behavior of the system because of its simplicity. The accuracy of the technique is more than sufficient for engineering purposes. The piece-wise linearization method was used to gain further insight into determining the oscillatory modes. It was not necessary to introduce the Z-transform into the analysis to represent the effect of the sampler. Although the phase plane method was not employed extensively, this method may prove to be more useful in the analysis of the system response to larger acceleration inputs.

Analytic and graphical procedures for determining the oscillatory modes of the accelerometer modes were presented in Chapter III. A heuristic extension of these procedures provided an explanation of the response of the system to small inputs in Chapter IV. Based upon the analysis, design criteria to be used in the systhesis of a pulse restrained accelerometer are given in Chapter V. An analog computer simulation and laboratory experiments substantiated the analytic development.

Having described the moding existing in this sample data contactor feedback control system and the deadzone resulting from the presence of elastic restraint, any further work should be directed toward determining the system response to large inputs. Inputs other than step functions should be considered and the effect of the amplitude and frequency of the acceleration input upon the

accuracy of the velocity information should be investigated. Having available the analytic techniques of this report, computer simulation and laboratory experiments appear to be suitable means for future investigations.

APPENDIX

Analog Computer Simulation

A.1 Computer Program

The experimental accelerometer which was simulated on the analog computer has the following parameters:

$$\tau_2 = \frac{I}{C} = .43 \times 10^{-3} \text{ sec.}$$

$$\tau_1 = \frac{C}{K} = 12.5 \text{ sec.}$$

$$\pm M = \pm 5 P_g$$

$$\frac{K'}{P_g} = 8$$

The scale factors which were required to reduce the basic system equations to computer equations are as follows:

$$t_{computer} = \frac{t_{actual}}{1000}$$

$$5 \times 10^4 \text{ volts} = 1 \text{ radian}$$

Neglecting the elastic restraint which is too small to simulate on the computer, the following differential equation was programmed to represent the pendulum:

$$\ddot{\theta} + 2.33\dot{\theta} = \pm 5.8 \text{ volts}$$

The program is shown in Figure A.1. The Schmitt trigger served as the contactor and the sample-and-hold operation was performed by a flip-flop gated by clock pulses.

A.2 Discussion of Simulation Results

A typical trajectory in the phase plane is shown in Figure A.2. The system is initially in a 2:2 mode and an acceleration step input is applied at point A so that the average value of the pendulum "limit cycle" moves off to the right

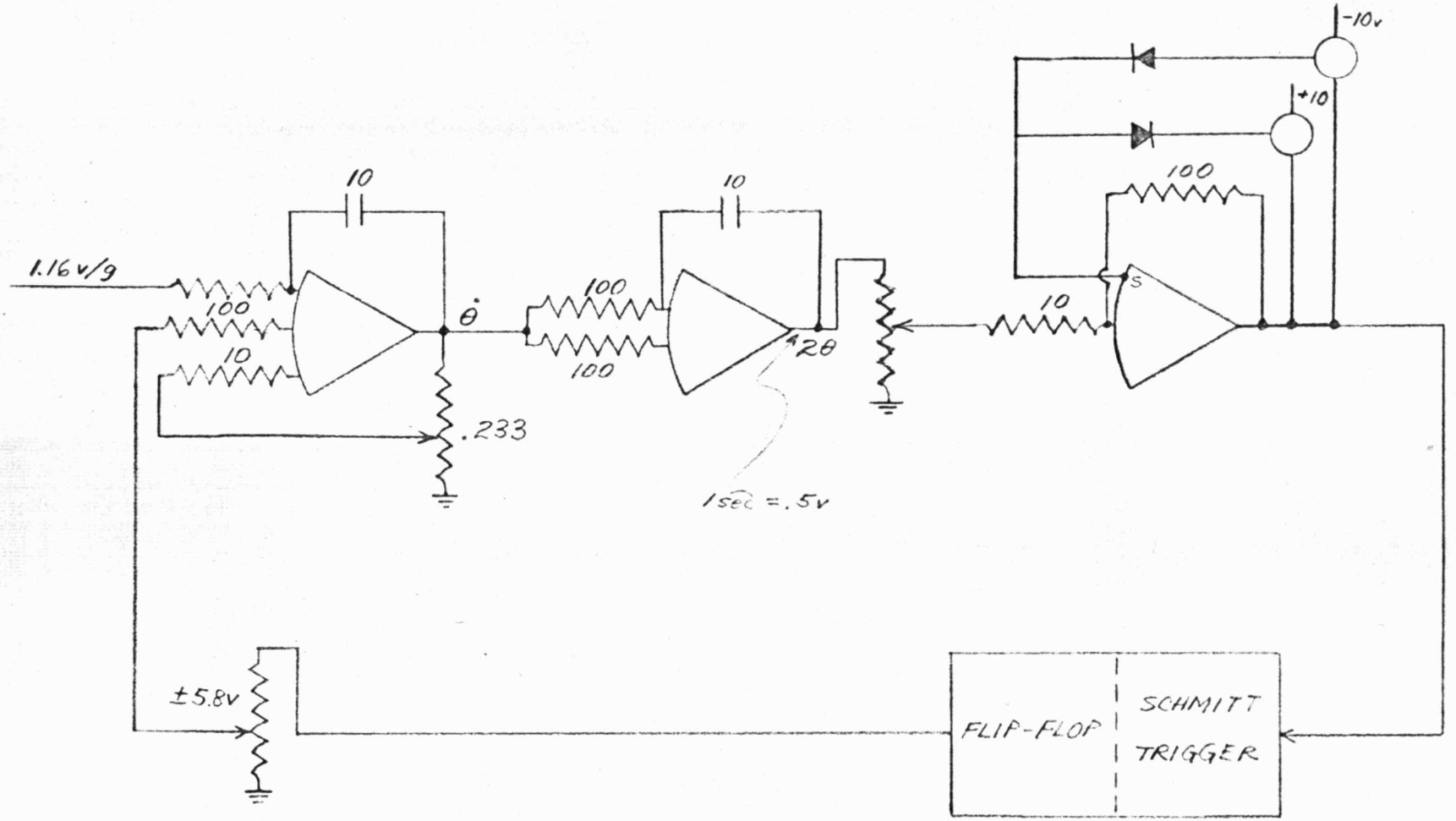

FIGURE A.1

ANALOG COMPUTER PROGRAM

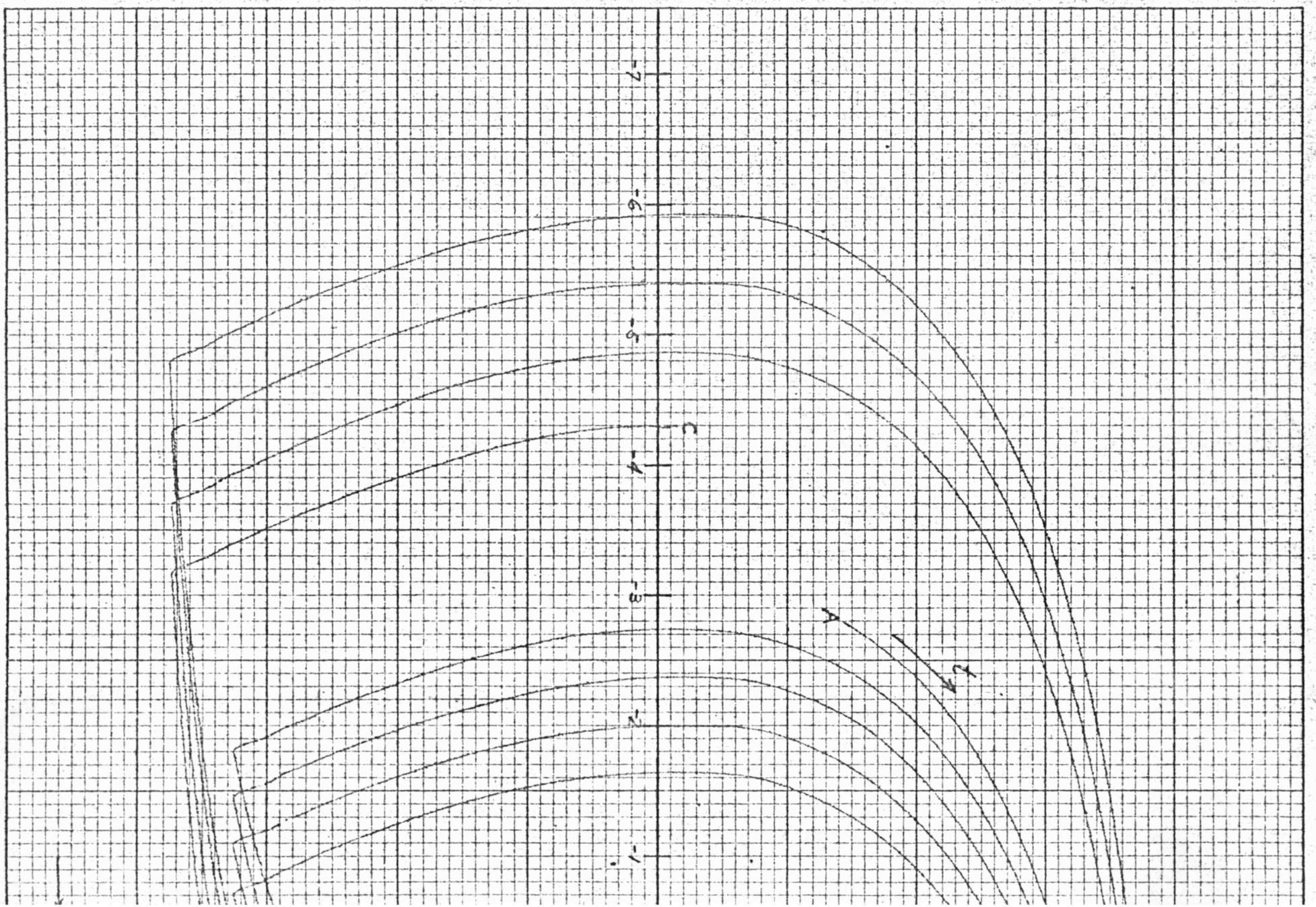

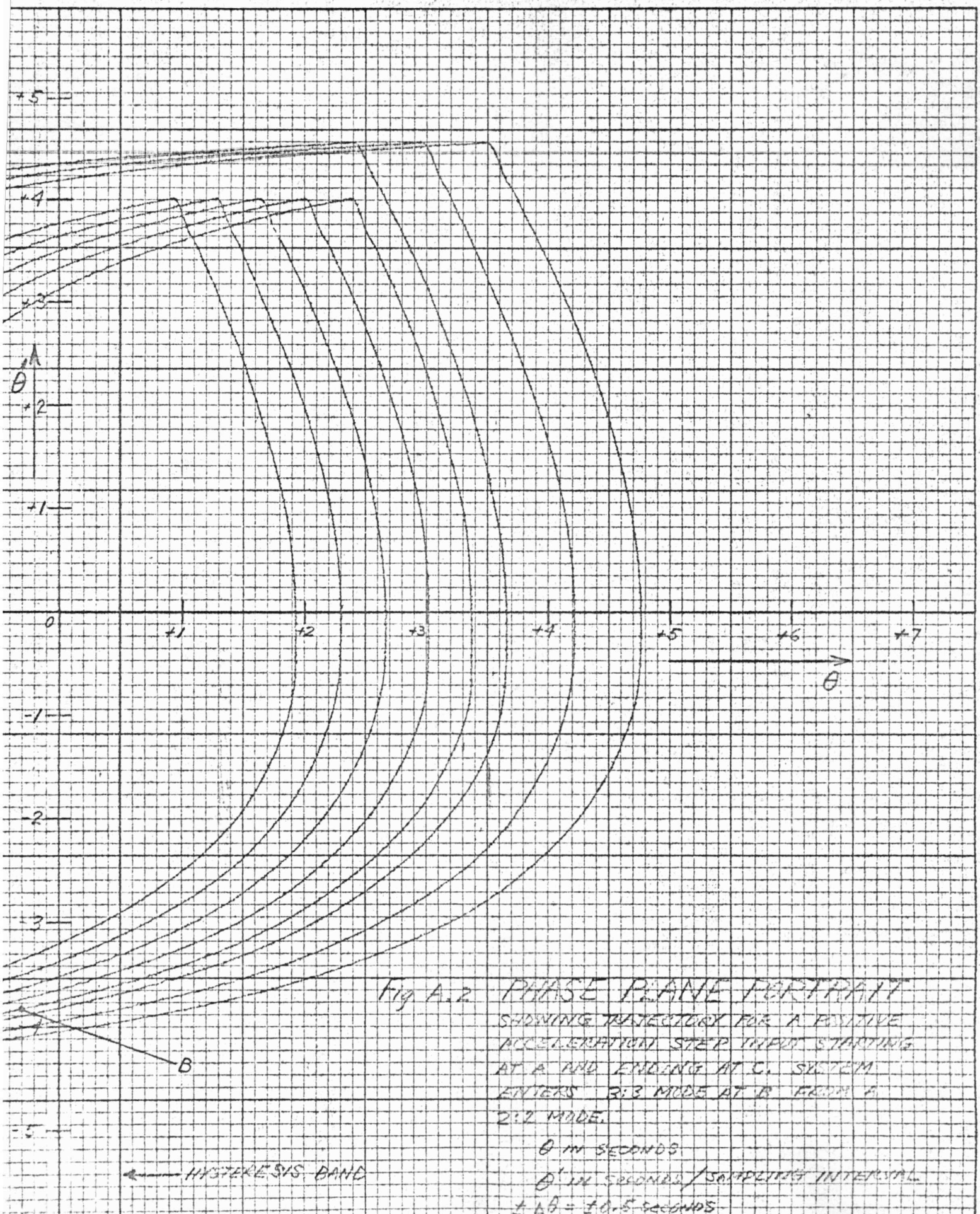

Fig A.2 PHASE PLANE PORTRAIT

SHOWING TRAJECTORY FOR A POSITIVE ACCELERATION STEP INPUT STARTING AT A AND ENDING AT C. SYSTEM ENTERS 3:3 MODE AT B FROM A 2:2 MODE.

θ IN SECONDS

$\dot{\theta}$ IN SECONDS / SAMPLING INTERVAL

$\pm \Delta\dot{\theta} = \pm 0.5$ SECONDS

at a constant rate. At point B, the torque should reverse if the system is to remain in the 2:2 mode. Since B is within the hysteresis band, the trajectory continues on to the left and thus enters a 3:3 mode. If the step input were to remain applied, the system would continue to switch between the two modes.

For very small inputs the system switches betwen the 2:2 and 3:3 modes at a rate proportional to the input as can be seen in Figure A.3 and A.4. The torque feedback signal existing for 1g, 3g and 4g step inputs are periodic in Figures A.5, A.7 and A.8 because the amplitude of the feedback signal is 5g's, an integer multiple of the input.

This periodic behavior of the torque feedback signal would be impossible for smaller inputs, even though 5g's is an integer multiple of the input because the shorter of the two torque half cycles must consist of three or less pulses. (Since a 4:4 mode could not be sustained with a zero input, a torque half cycle of four pulses can not exist in the presence of an acceleration input which is tending to drive the pendulum toward its reference position during the shorter torque half cycle.)

For inputs, of which 5g's is not an integer multiple, the system may have a periodic behavior which lasts for several cycles as the average value of the "limit cycle" moves away from the reference position until a pulse is "gained" as shown in Figure A.9. The periodic behavior may correspond to a higher acceleration so that a pulse is "lost" every few cycles as the average value of the "limit cycle" moves toward the reference position, as in Figure A.10.

The effect of a change in the sampling rate is shown in Figures A.12, A.13, A.14 and A.15a. An increase in the clock rate results in a smaller instantaneous velocity error as the time required to detect an incremental change in velocity is decreased.

If the contents of the up-and-down counter are put into the velocity accumulator at the end of every positive torque half cycle, a net output of one ΔV pulse occurs at point A in Figure A.13 as the counter is cleared for the next torque cycle. Even though there is a change in mode at point B, there is no net output since the mode change is "in phase" with the counter. The next output does not occur until point C is reached.

The addition of elastic restraint ($\tau_1 = \frac{C}{K} = .01655$ sec.) caused the pendulum response to change from that of Figure A.15b to that of Figure A.16. The average value of the "limit cycle" in Figure A.16 moves away from the reference position to the position where the torque due to the acceleration input is balanced by the elastic restraint torque. Since this steady state value is less than the mode switching angle, no incrememtal change in velocity is detected.

In addition to preventing the detection of acceleration within the dead-zone, elastic restraint affects the linearity of the system outside the dead-zone. When the integrator time constant ($\frac{C}{K}$) was increased to .0233 seconds in Figure A.17, the mode changed and therefore resulted in an indication of ΔV. However, the average value of the "limit cycle" approached the mode switching angle exponentially due to the integrator time constant. This caused the mode switching to occur at point B rather than at point A. This time lag causes an unrecoverable velocity error of ($t_B - t_A$) times the acceleration input.

The situation where the mode changes without producing an output was substantiated in the computer simulation. With a very small input being

applied to the pendulum in Figure A.18, the system went through a -2, +3, -3, +2 sequence in going from the 3:3 to the 2:2 modes. Later a +3, -2, +2, -3 sequence occurs as the system changes from the 2:2 to the 3:3 mode. The presence of the very small g input prevented the sequence from occurring more than once each time the mode changed. Not only is this type of "limit cycle" unstable, the range of initial conditions for its existance is very small.

Bibliography

1. Graham and McRuer, Analysis of Nonlinear Control Systems, (book) John Wiley and Sons, New York, 1961.

2. Hazen, Harold J., Theory of Servomechanisms. Journal, Franklin Institude, Vol. 218, No. 3, Sept. 1934, pages 279-330.

3. Kahn, David A., An Analysis of Relay Servomechanisms, AIEE Trans., Vol. 68, 1949, pages 1079-1088.

4. Bergen, A. R., discussion following Reference 5. pages 304-305.

5. Torng, H. C. and Meserve, W. E., Determination of Periodic Modes in Relay Servomechanisms Employing Sampled-Data, IRE Trans. on Automatic Control, Vol. AC-5, No. 4, Sept. 1960, pages 298-305.

6. Weiss, H. K., Analysis of Relay Servomechanisms, Journal, Aero. Sciences, Vol. 13, July 1946, pages 364-376.

7. MacCall, LeRoy A., Fundamental Theory of Servomechanisms, (book), D. Van Nostrand Co., New York, 1945.

8. Minorsky, N., Introduction to Non-Linear Mechanics, (book), J. W. Edwards, Ann Arbor, Michigan, 1947.

9. Andronow, A. A. and Chaikin, C. E., Theory of Oscillations, (book), Moscow, 1937, English edition, Solomon Lefschitz, Princeton University Press, New Jersey, 1949.

10. Kalman, Rudolph E., Phase-Plane Analysis of Non-Linear Sampled Data Systems, M. S. Thesis, M. I. T., 1954.

11. Mullin, F. J, and Jury, E. I., A Phase-Plane Approach to Relay Sampled-Data Feedback Systems, AIEE Trans., Vol. 78, Jan. 1959, pages 517-523.

12. Kochenburger, Ralph J., A Frequency Response Method for Analyzing and Synthesizing Contactor Servomechanisms, AIEE Trans., Vol. 61, 1950, pages 270-284.

13. Chow, C. K., Contactor Servomechisms Employing Sampled Data, Ph. D. Thesis, Cornell University, 1954.

14. Chao, Stanley K., A Design of a Contactor Servo Using Describing Function Theory, AIEE Trans., Sept. 1956.

15. Gelb, Arthur, The Analysis and Design of Limit Cycling Adaptive Automatic Control Systems, D.Sc. Thesis, M.I.T., 1961.

16. Hutchings, Patrick B. Jr., Compensation of a Sample Data Contactor Servo, M.S. Thesis, M. I. T., 1959.

17. Schwartz, Stuart C., Analysis of Sampled-Data Relay Servomechanisms with Zero and Step Inputs, M.S. Thesis, M. I. T., 1961.

18. Izawa, K. and Weaver, L. E., Relay-Type Feedback Control Systems with Dead Time and Sampling, AIEE Trans., May 1959.

19. Jury, E. I. and Nishimura, T., On the Periodic Modes of Oscillations in Pulse-Width Modulated Feedback Systems, AFOSR-TN-60-1474, University of California Electronics Research Laboratory, Nov. 1960.

20. Weiner, Thomas F., unpublished D.Sc. thesis, M.I.T., 1961.

21. Theiss, C. M., The Theory and Analysis of a Digital Accelerometer, Technical Memorandum BEF-101, AC Spark Plug Div., Wakefield, Mass., 1960.

22. Theiss, C. M., The Pulse Torqued Accelerometer, Technical Memorandum BEF-102, AC Spark Plug Div., Wakefield, Mass., 1961.

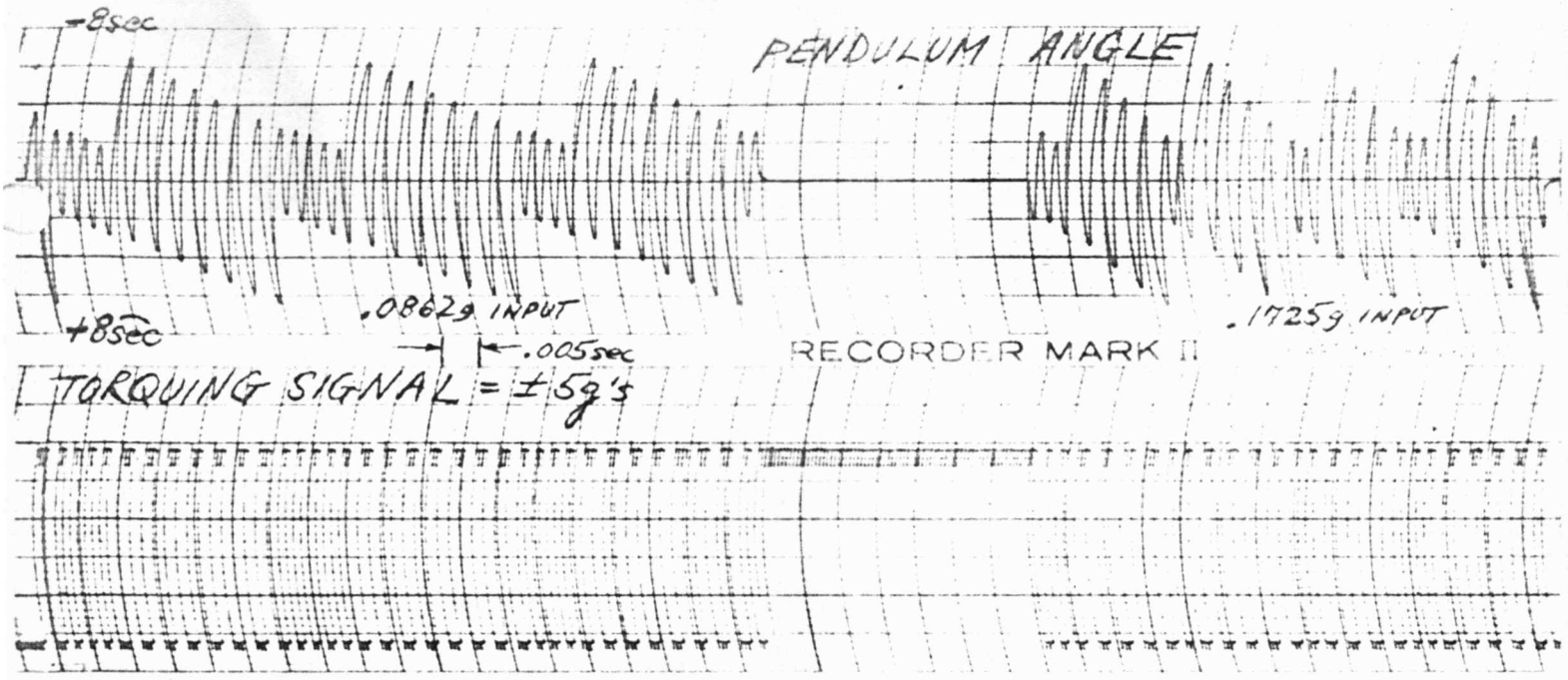
-8sec
PENDULUM ANGLE
+8sec
.0862g INPUT
.005sec
.1725g INPUT
RECORDER MARK II
TORQUING SIGNAL = ±5g's

A.3

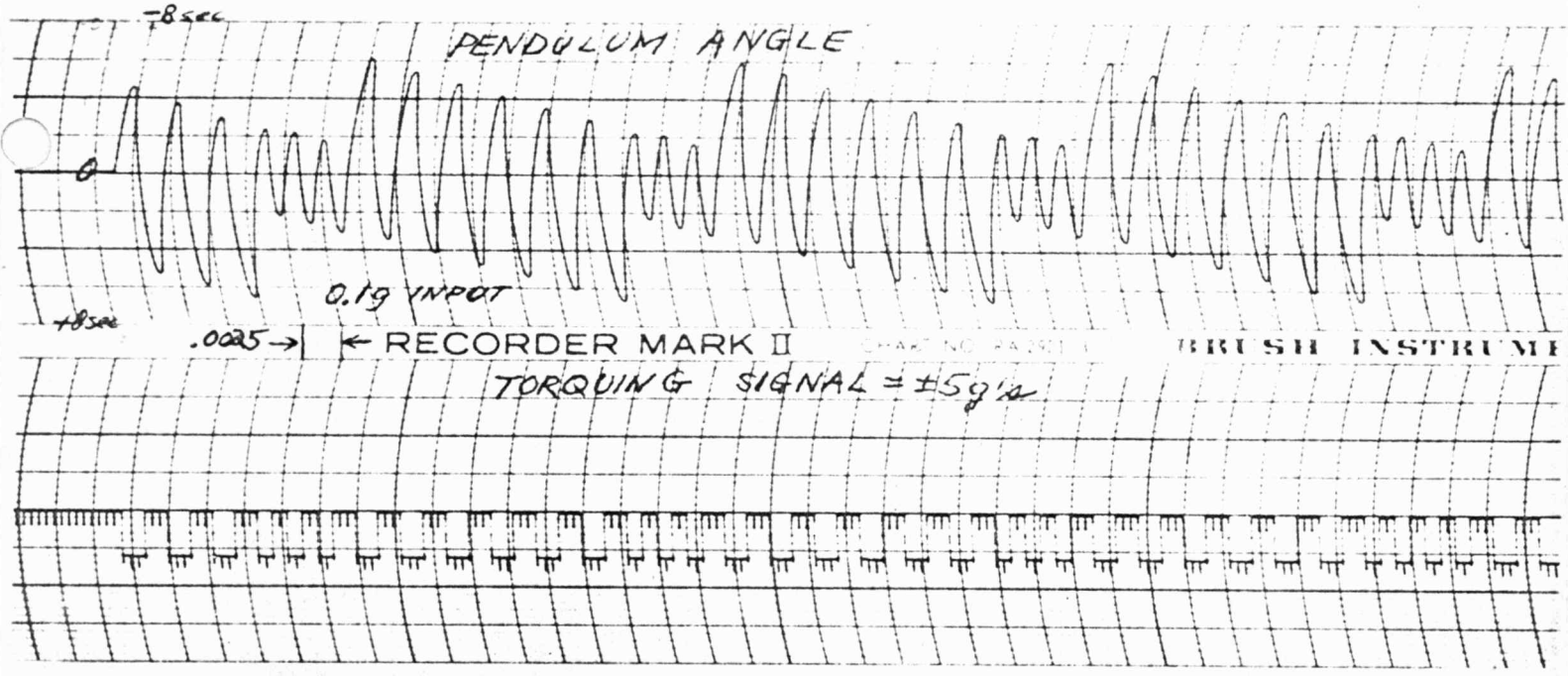
-8sec
PENDULUM ANGLE
0
0.1g INPUT
+8sec
.0025
RECORDER MARK II
TORQUING SIGNAL = ±5g's

A.4

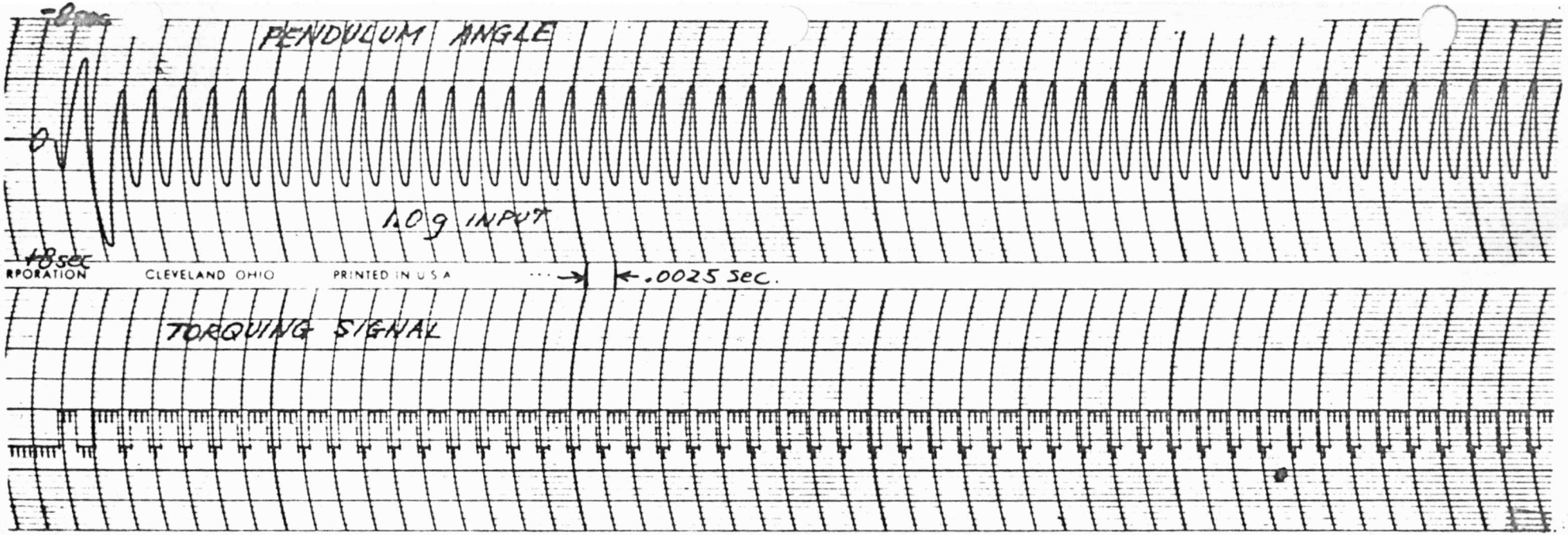
PENDULUM ANGLE
1.0g INPUT
CLEVELAND OHIO
PRINTED IN U.S.A.
.0025 Sec.
TORQUING SIGNAL

A.5

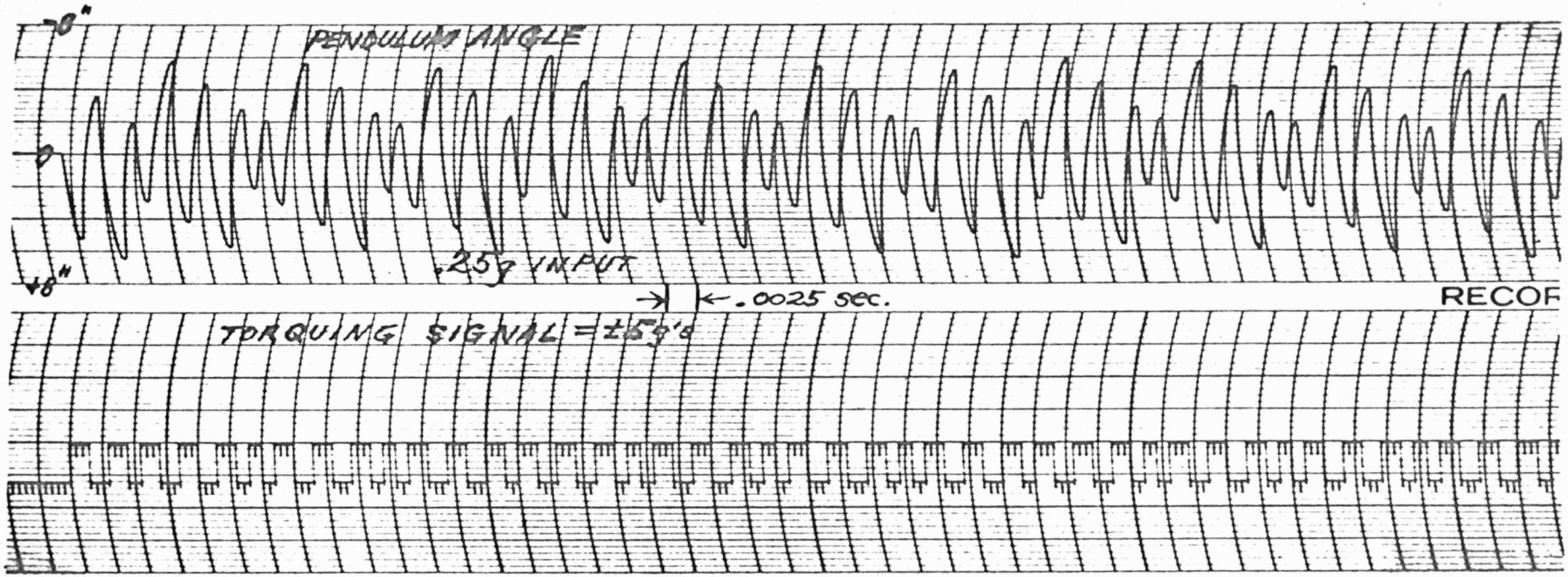
PENDULUM ANGLE
.25g INPUT
.0025 sec.
TORQUING SIGNAL = ±5g's

A.6

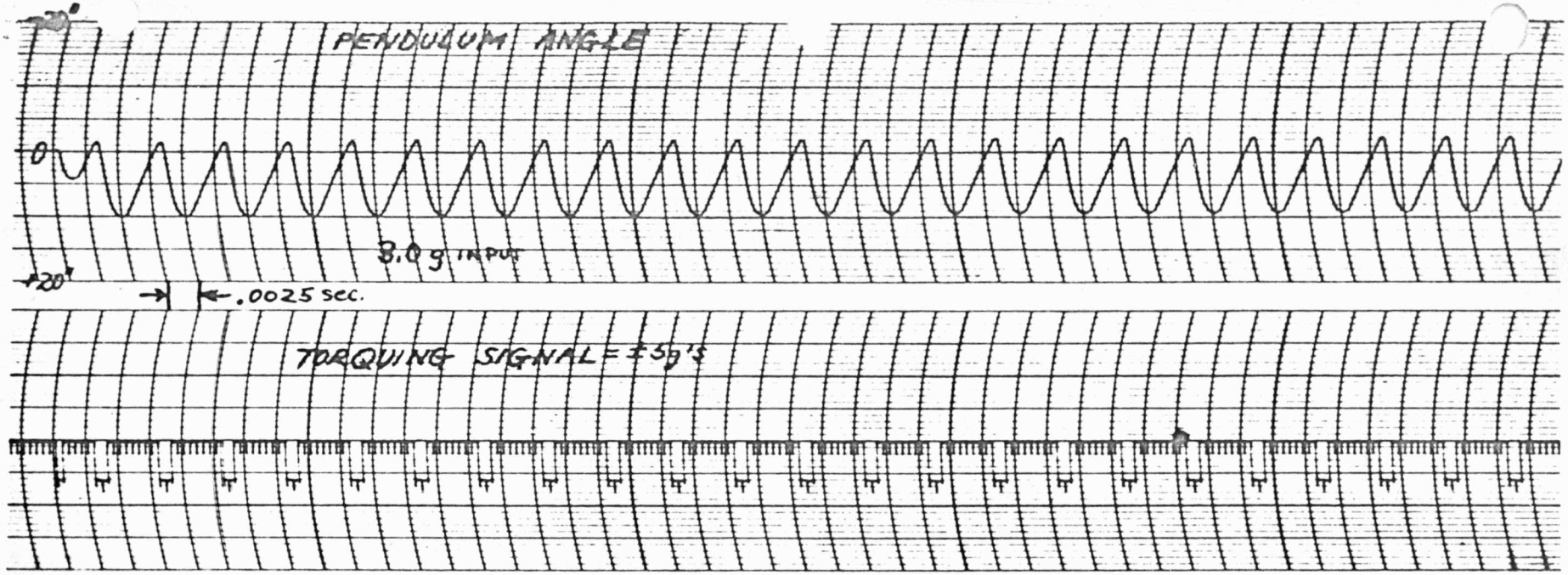
PENDULUM ANGLE
0
3.0 g INPUT
.0025 sec.
TORQUING SIGNAL = ±5g's

A.7

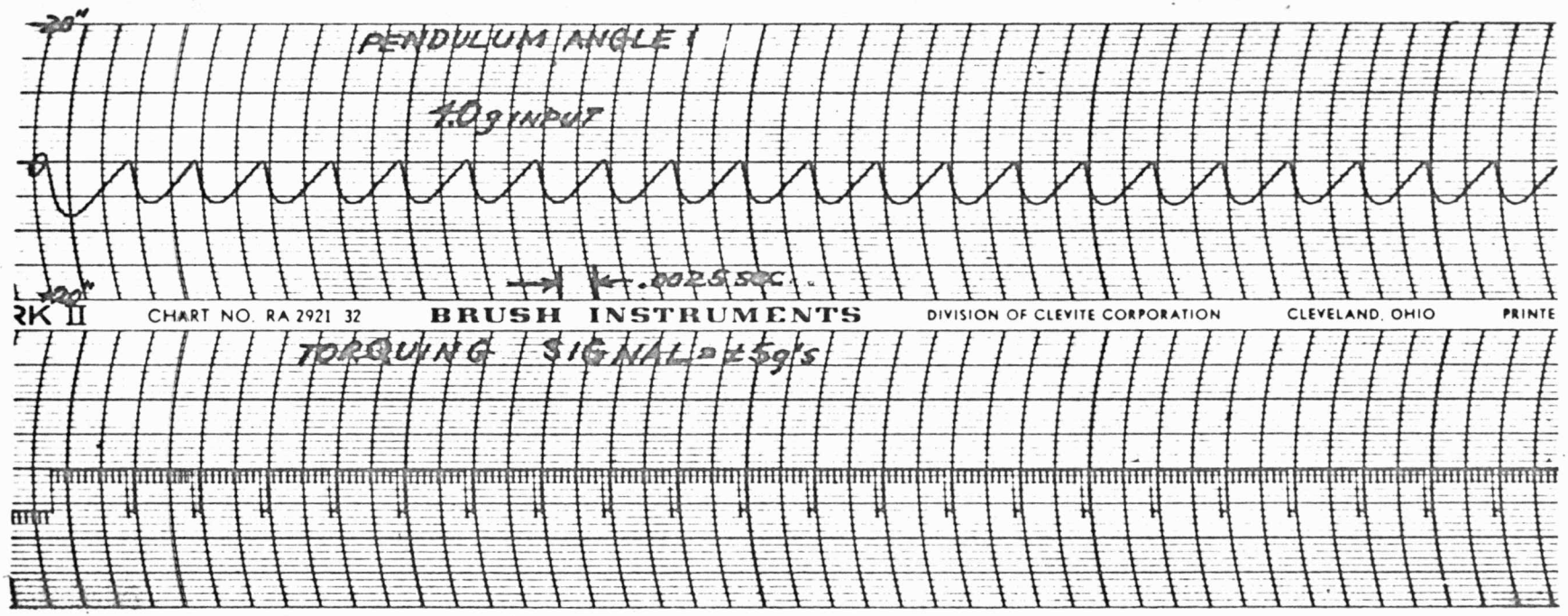
PENDULUM ANGLE
1.0g INPUT
0
.0025 SEC.
CHART NO. RA 2921 32
BRUSH INSTRUMENTS
DIVISION OF CLEVITE CORPORATION
CLEVELAND, OHIO
TORQUING SIGNAL = ±5g's

A.8

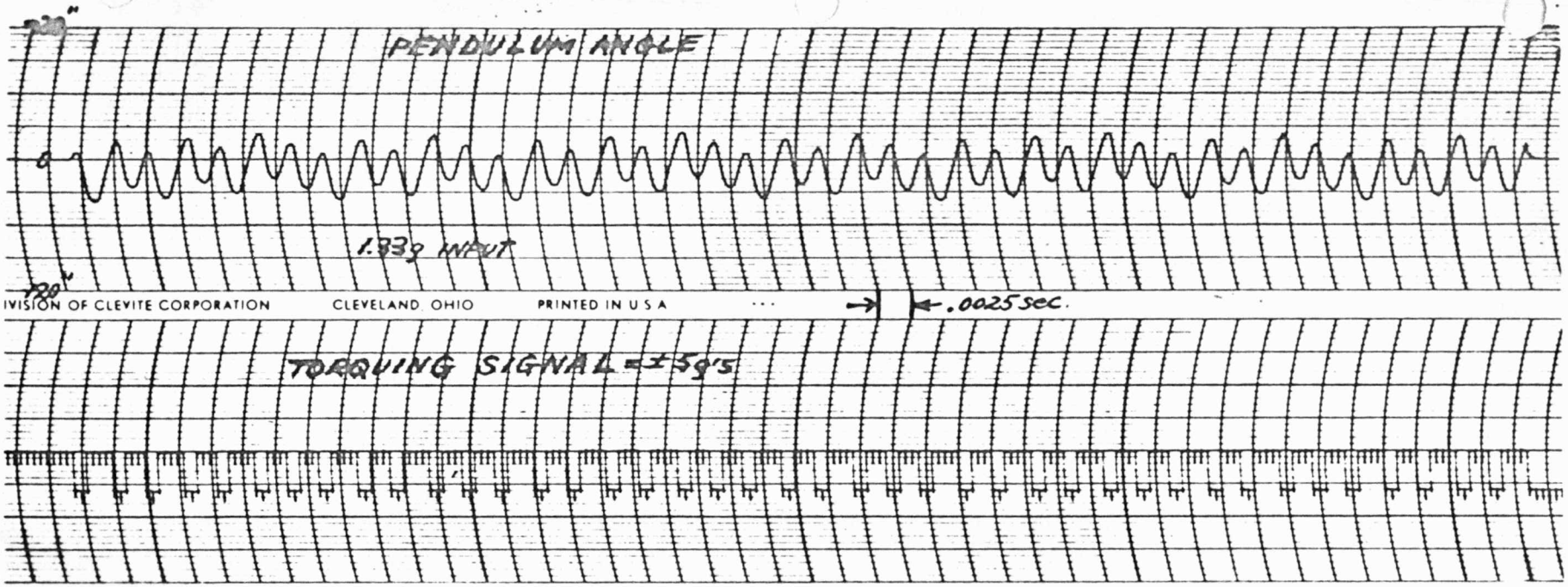
PENDULUM ANGLE
0
1.33g INPUT
IVISION OF CLEVITE CORPORATION CLEVELAND OHIO PRINTED IN U S A
.0025 sec.
TORQUING SIGNAL = ±5g's

A.9

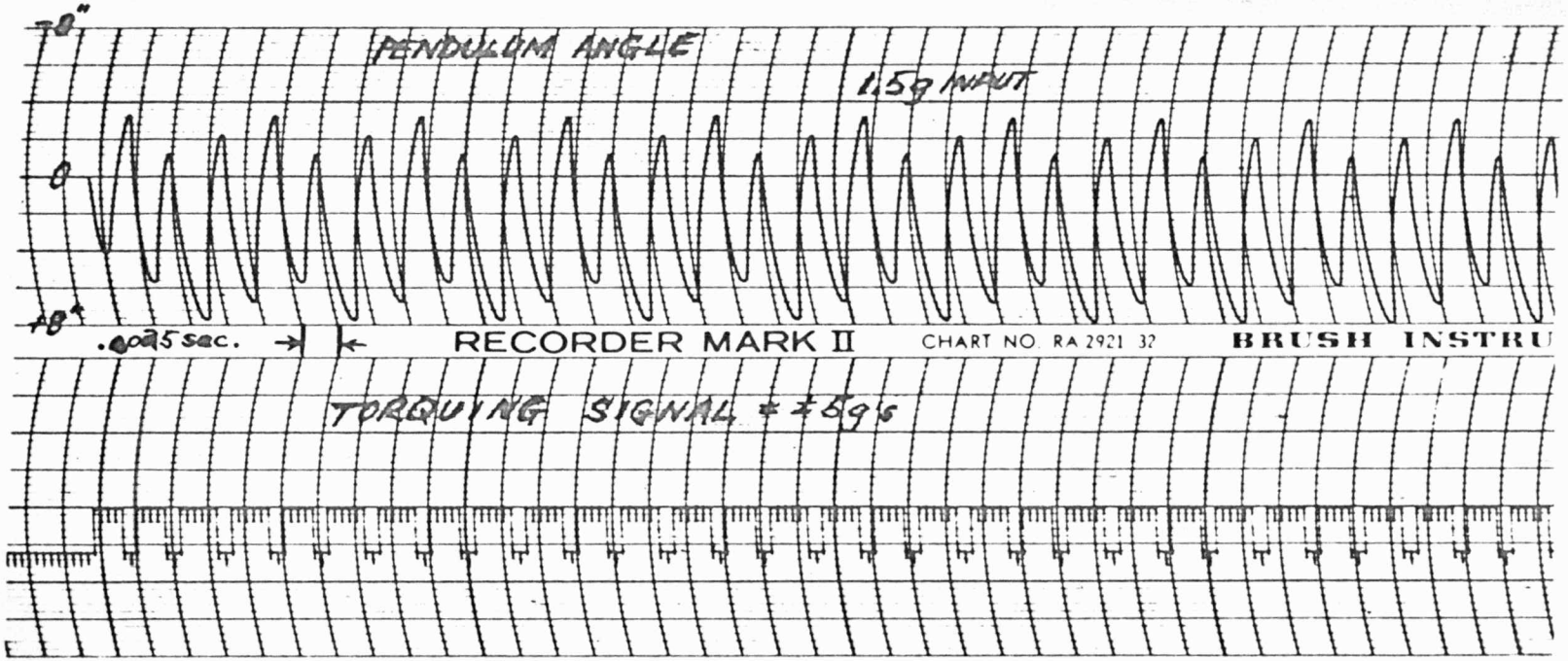
PENDULUM ANGLE
1.5g INPUT
0
.0025 sec.
RECORDER MARK II
CHART NO. RA 2921 32
BRUSH INSTRU
TORQUING SIGNAL = ±5g's

A.10

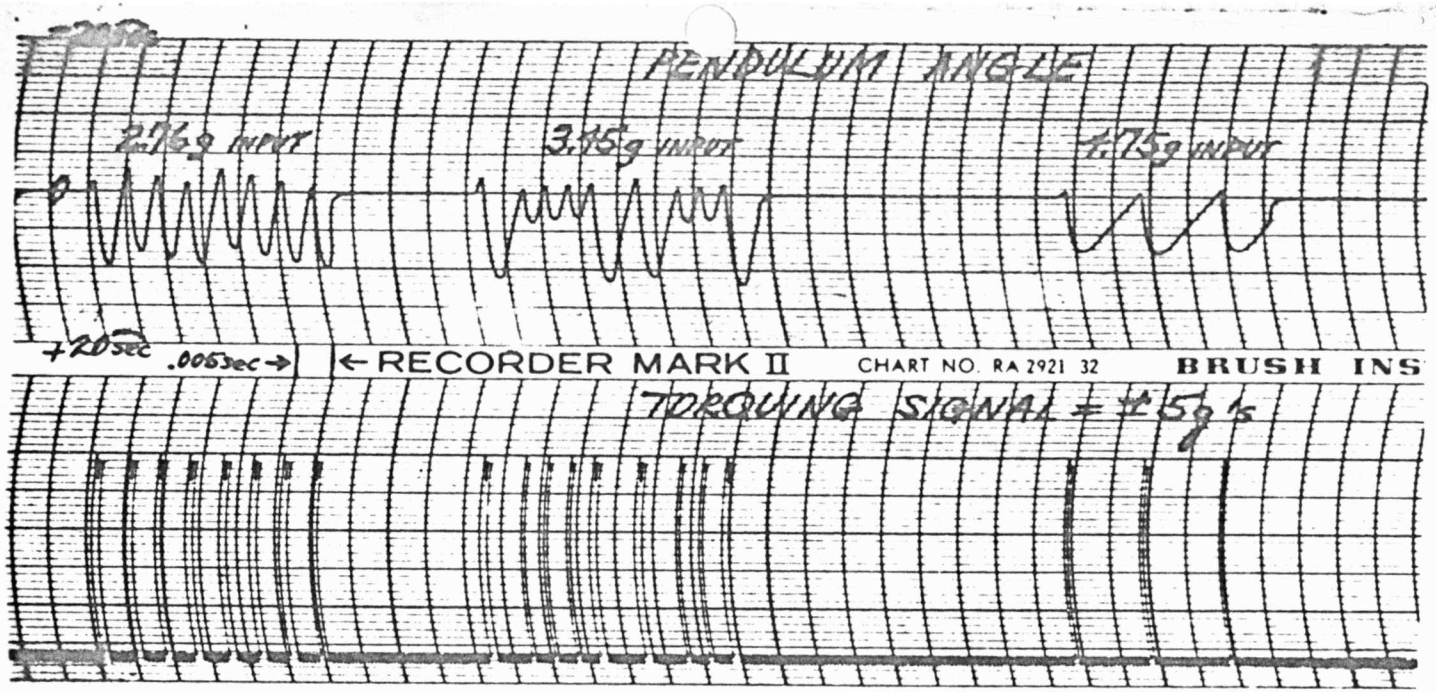
PENDULUM ANGLE
2.76g INPUT
3.45g INPUT
4.75g INPUT
0
+20sec
.005sec
RECORDER MARK II
CHART NO. RA 2921 32
BRUSH INS
TORQUING SIGNAL = ±5g's

A.11

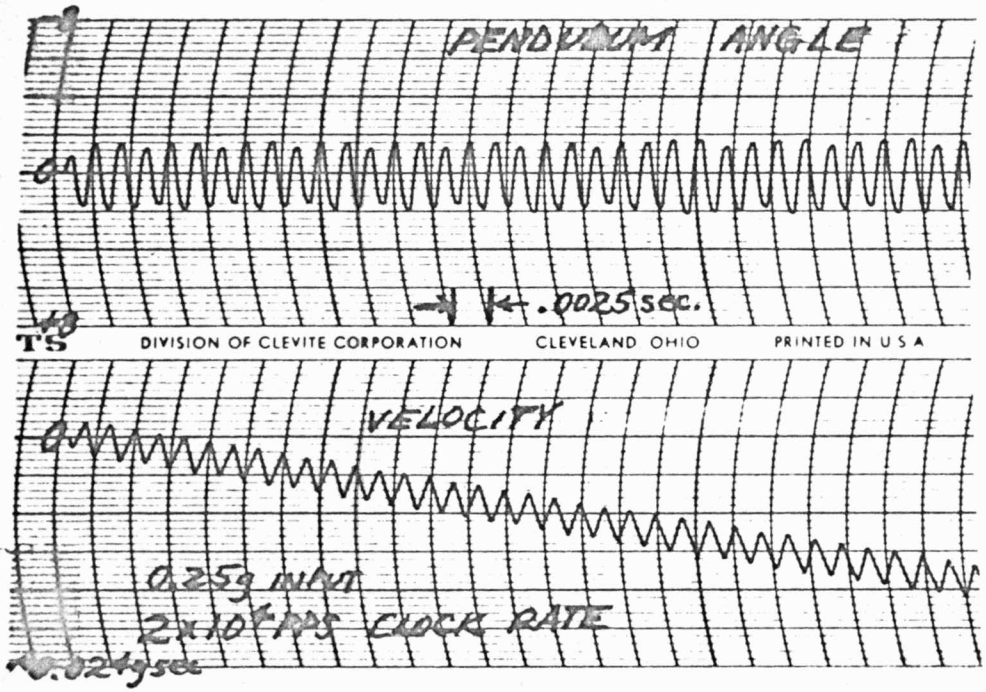
PENDULUM ANGLE
0
.0025sec.
TS
DIVISION OF CLEVITE CORPORATION
CLEVELAND OHIO
PRINTED IN U S A
VELOCITY
0.25g INPUT
2x10³PPS CLOCK RATE
.024sec

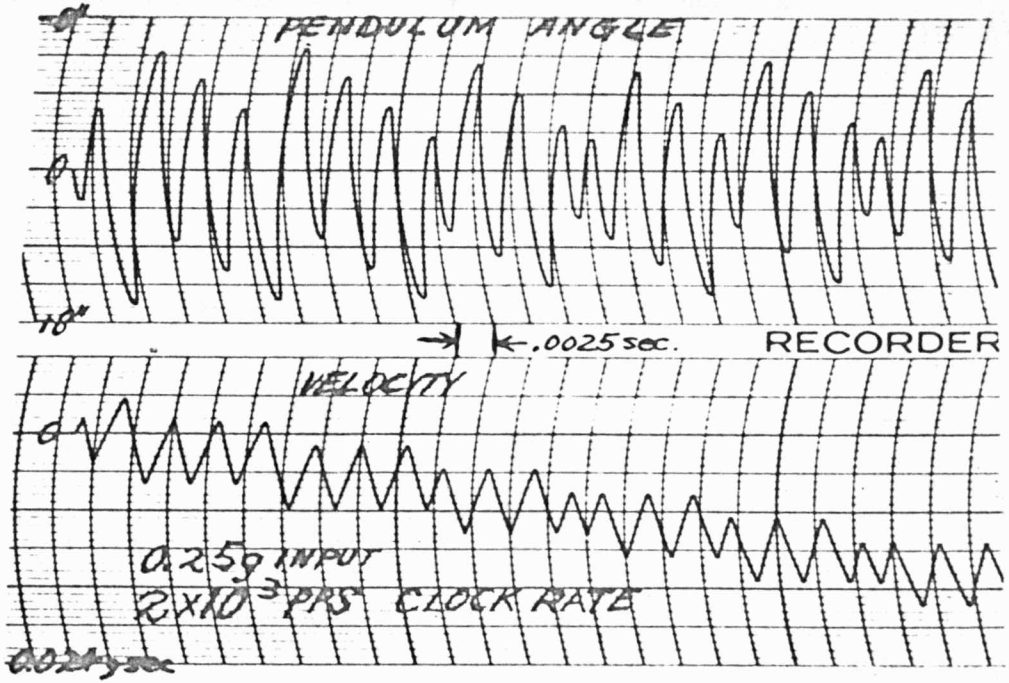
PENDULUM ANGLE
0
18"
.0025sec.
RECORDER
VELOCITY
0.25g INPUT
2x10³PPS CLOCK RATE
.024sec

A.12

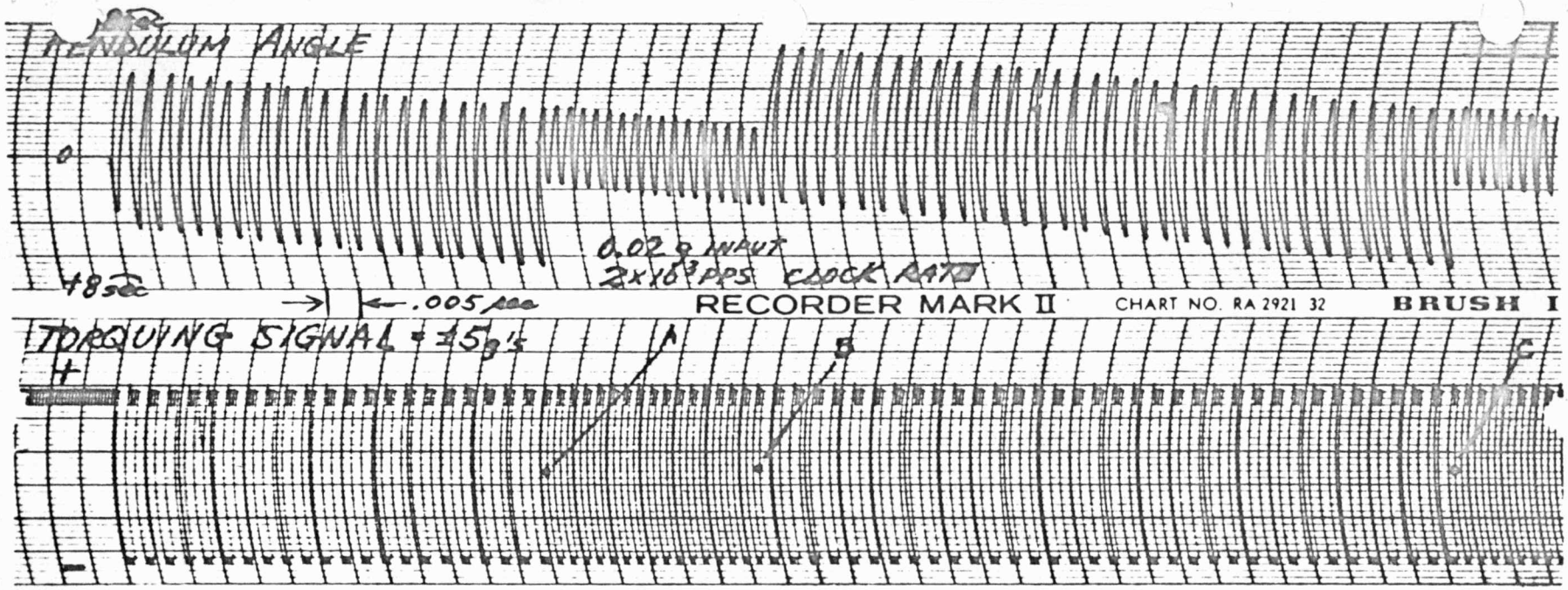
PENDULUM ANGLE
0
0.02 g INPUT
2x10³ PPS CLOCK RATE
.48sec
.005sec
RECORDER MARK II
CHART NO. RA 2921 32
BRUSH I
TORQUING SIGNAL = ±15g's
+
A
B
C
-

A.13

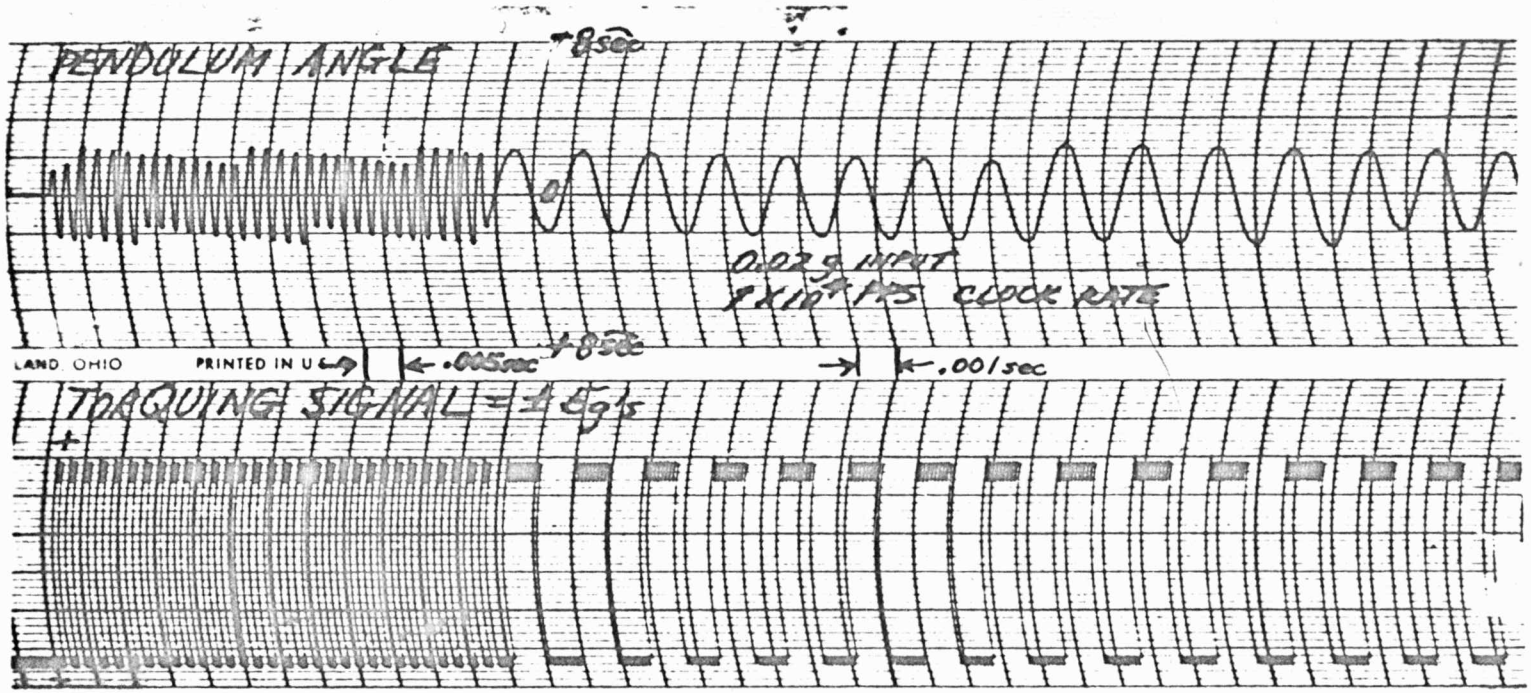
PENDULUM ANGLE
.8sec
0
0.02 g INPUT
2x10³ PPS CLOCK RATE
LAND, OHIO
PRINTED IN U
.005sec
.8sec
.001sec
TORQUING SIGNAL = ±15g's
+

A.14

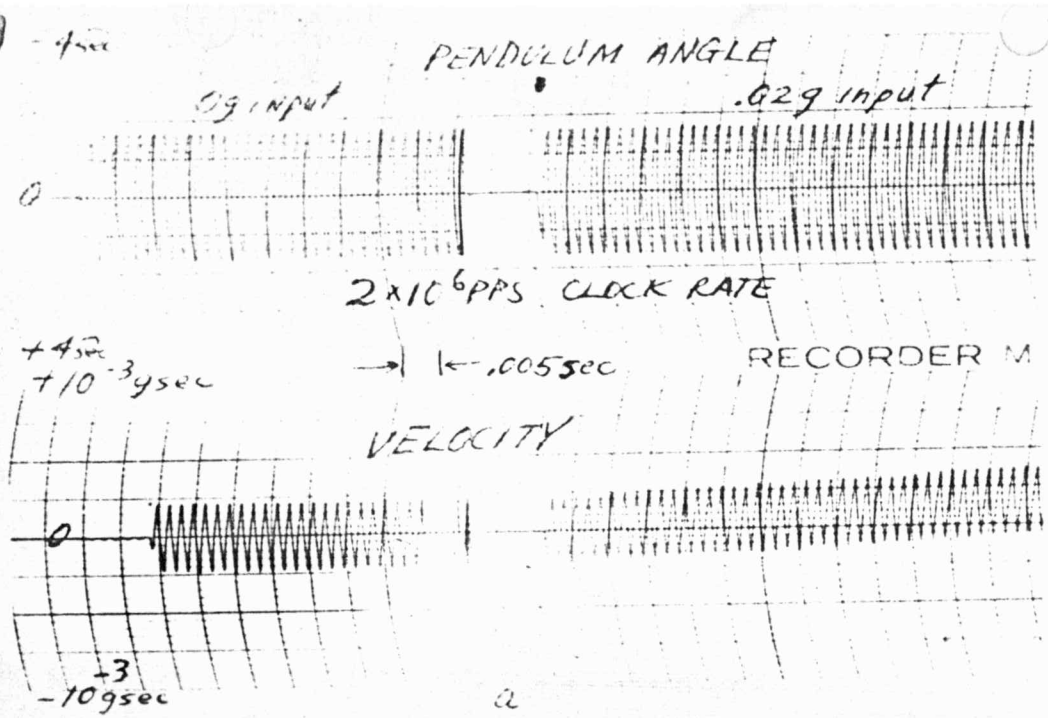
PENDULUM ANGLE
0g input
.62g input
0
2 x 10^6 PPS CLOCK RATE
+4sec
+10^-3 g sec
.005 sec
RECORDER M
VELOCITY
0
+3
-10 g sec
a

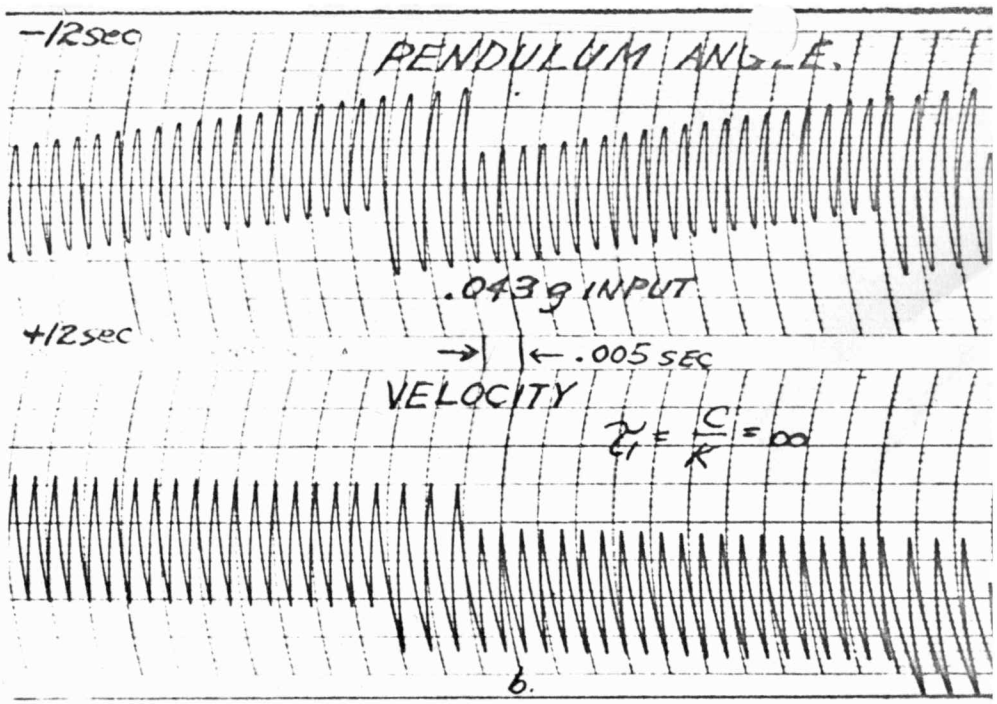
-12sec
PENDULUM ANGLE
.043g INPUT
+12sec
.005 SEC
VELOCITY
τ = C/K = ∞
b.

A.15

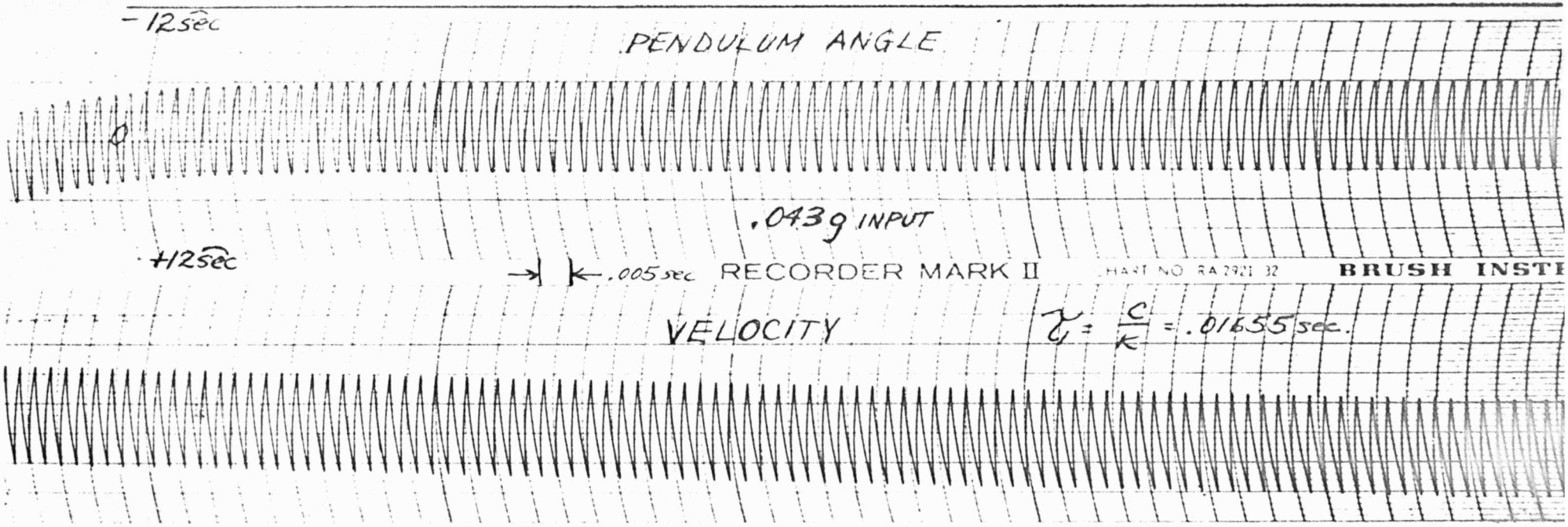
-12sec
PENDULUM ANGLE
0
.043g INPUT
+12sec
.005 sec RECORDER MARK II
CHART NO RA 2921 32
BRUSH INSTR
VELOCITY
τ = C/K = .01655 sec.

A.16


PENDULUM ANGLE
.043g input
RECORDER MARK II
CHART NO. RA 2921 32
TORQUING SIGNAL = ± 5 V's

A.17

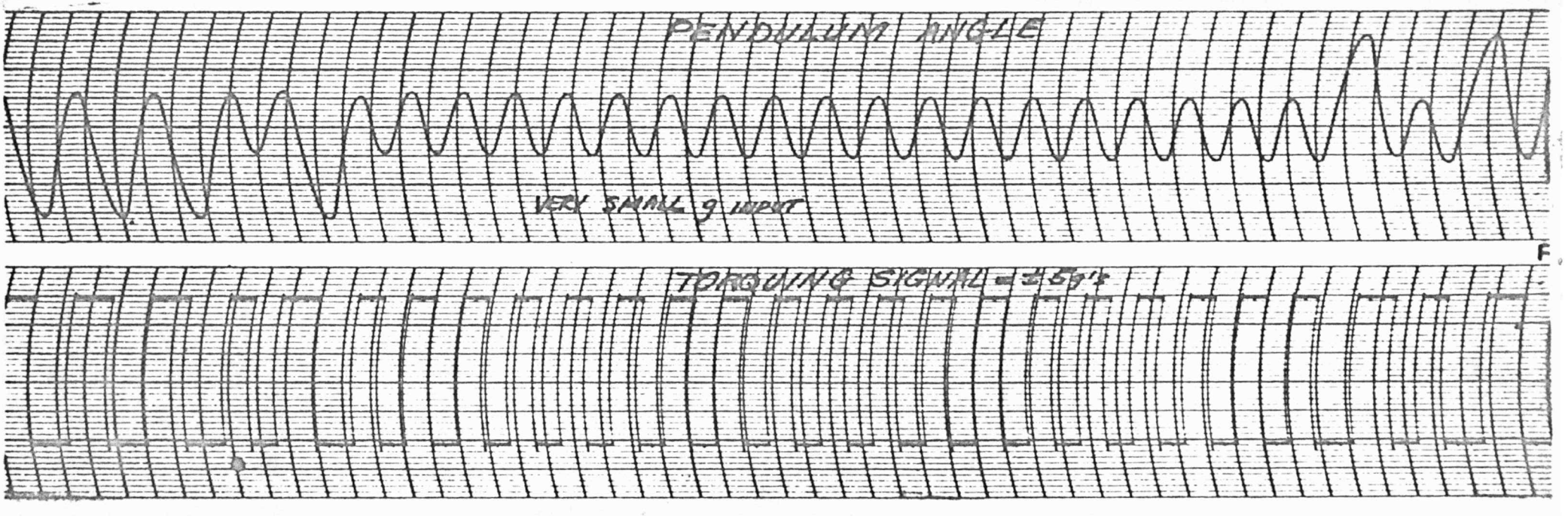
PENDULUM ANGLE
VERY SMALL g INPUT
TORQUING SIGNAL = ± 5 V's

A.18